ORGANOMETALLICS

Article

Cite This: Organometallics XXXX, XXX, XXX−XXX

When Applying the Mercury Poisoning Test to Palladacycle-Catalyzed Reactions, One Should Not Consider the Common Misconception of Mercury(0) Selectivity

Olga N. Gorunova,[†] Ivan M. Novitskiy,[‡] Yuri K. Grishin,[‡] Igor P. Gloriozov,[‡] Vitaly A. Roznyatovsky,[‡] Victor N. Khrustalev,[§,∥] Konstantin A. Kochetkov,[†] and Valery V. Dunina*[,‡]

[†]A. N. Nesmeyanov Institute of Organoelement Compounds, Russian Academy of Sciencies, Vavilova St. 28, 119991 Moscow, Russian Federation

[‡]Department of Chemistry, M. V. Lomonosov Moscow State University, Lenin Hills, 119991 Moscow, Russian Federation

[§]Inorganic Chemistry Department, Peoples' Friendship University of Russia, Miklukho-Maklay Street 6, 117198 Moscow, Russian Federation

[∥]National Research Center, Kurchatov Institute, Acad. Kurchatov Sq. 1, Moscow 123182, Russian Federation

Supporting Information

ABSTRACT: The aim of this study was to demonstrate the absolute necessity of control experiments for a correct interpretation of mercury drop test results when applied to mechanistic studies of palladacycle-catalyzed reactions. It was shown that the interaction of diverse azapalladacycles with metallic mercury leads to the formation of organomercuric chlorides during the redox-transmetalation process. The structure of these organomercurials was confirmed by elemental analysis, ^{1}H, ^{13}C{^{1}H}, and ^{199}Hg{^{1}H} NMR spectra, X-ray diffraction analysis, and DFT calculations. The behavior and properties of *C,N*-mercuracycles bearing the weak and labile N···Hg bond are discussed on the basis of the temperature dependence of the NMR spectra and calculated thermodynamic parameters of the dechelation process.

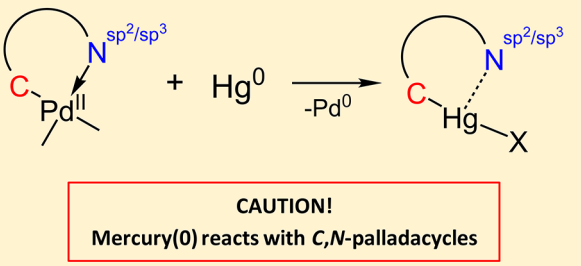

INTRODUCTION

The success of catalytic system development is dependent on a clear understanding of the reaction mechanism and the nature of the true catalyst. Among a rather rich collection of diagnostic tools proposed to explore this issue,[1,2] the mercury poisoning test is the most popular due to its easy procedures. This method, known for almost a century,[3] was first based on the ability of mercury(0) to amalgamate zero-valent metals or to adsorb on the metal surface.[4] The interpretation of mercury poisoning results has significantly changed over time. Initially, this test was considered a way to distinguish between homogeneous and heterogeneous catalysts; the suppression of the reaction by excess metallic mercury served as evidence for heterogeneous catalysis.[5] Later, Schwartz suggested using more mechanistically oriented terms: "homotopic and heterotopic" catalysis, depending on the nature of the catalytic sites, not on the phases involved.[6] However, this reasonable terminology is still almost never used. The next step in the interpretation of mercury(0) poisoning results was made by Jones,[1c,7] who suggested relating the results of the test for palladium-catalyzed cross-coupling reactions with the type of catalytic cycle as follows: "the observation that Hg(0) does not affect the catalysis can confirm a mechanism that does not involve unprotected Pd(0) (soluble or supported), whereas an observation that Hg(0) quenches the activity may be consistent with a Pd(0) intermediate".[1c] In support of this idea, it is useful to mention that there are several known examples of mercury(0) interaction with soluble molecular complexes of zero-valent metals, such as palladium, platinum, and rhodium.[8] Of course, the interaction of metallic mercury with metal complexes in elevated formal oxidation states bound by protective ligands usually is considered impossible.[1c,7,9]

Mechanistic studies are particularly important in the case of cross-coupling catalysis with cyclopalladated complexes (CPCs), palladacycles, or pincer palladabicycles, which have remained a subject of debate until now. In contrast to the widely accepted classic Pd(II)/Pd(0) pathway for these processes,[10] recent experimental[11] and theoretical investigations of these processes,[12] along with significant progress in the chemistry of cyclometalated palladium(IV) complexes,[13] have provided evidence in favor of alternative Pd(II)/Pd(IV) catalytic cycle viability. The most valuable and quite convincing experimental confirmation of the Pd(II)/Pd(IV) pathway for the intra-

Received: May 28, 2018

DOI: 10.1021/acs.organomet.8b00363
Organometallics XXXX, XXX, XXX−XXX

molecular version of the Heck cross-coupling reaction has been provided by Vicente's recent research.[14]

As one would expect, the mercury poisoning test has been widely used to estimate the mechanism of cross-coupling processes, but the results have often been contradictory. In accordance with Jones's suggestion,[1c] the observations that mercury(0) has no effect on the Heck, Suzuki and related reactions catalyzed by *C,N*-,[11d,15] and *C,P*-palladacycles[16] or *N,C,N′*-,[17] *C,N,O*-,[14c,d] *C,N,S*-,[11a] *C,N,Se*-,[18] *P,C,P*-,[19] and *S,C,S*-pincer complexes[11f] allow the exclusion of any catalytic cycles via the unprotected palladium(0) intermediates. However, in only a few studies, a logical homogeneous Pd(II)/Pd(IV) catalytic cycle[11a,d,f,19b] or homogeneous catalysis via molecular palladium(II) species[17,19a] was suggested. In Vicente's research,[14c,d] this conclusion was unambiguously confirmed by a rich set of additional testing experiments and ESI-MS detection of two palladium(IV) intermediates in the catalytic process. The opposite assumption about the homogeneous Pd(II)/Pd(0) pathway has been made in other reports[15,16] after a negative mercury drop test was obtained, despite the lack of an induction period in the kinetic curve[16] and the opportunity to regenerate and reuse the catalyst.[16a,b] Although the formation of strongly protected soluble palladium(0) species was not proven, it may be assumed in systems with *C,P*- or *P,C,P*-CPCs used as a (pre)catalyst. The rare exception is the research of Singh's team, who not only confirmed *C,N(S)*-palladacycle thermal decomposition under catalysis conditions and isolated and characterized in detail the nanoparticles (NPs) formed with Pd_7S stoichiometry but also established their homogeneous catalytic activity provided by palladium(0) atom leaching.[15]

More serious problems arise in the case of a positive mercury test. It was shown that mercury(0) suppresses (completely or partially)[20] the catalytic activity in cross-coupling reactions of palladium(II) cyclometalated *C,N*-,[20c,21] *C,P*-,[22] and *C,S*-complexes[23] and *P,C,P*-,[2b,7b,20a,b,24] *S,C,S*-,[7a,9b,25] *Se,C,Se*-,[26] and *C,N,*E (E = S, Se, Te)-pincers.[27] This result was considered by the authors as evidence of homogeneous catalysis with molecular palladium(0) species or colloidal palladium(0),[7a,b,9b,21e,f,22,24a] heterogeneous catalysis with palladium(0) nanoparticles (NPs),[2b,21a−d,23,24b,26] or a "cocktail" of homogeneous and heterogeneous pathways.[27,28] According to the Jones concept,[1c] a positive mercury test may be consistent with a catalytic cycle involving a palladium(0) intermediate. However, such a conclusion in some studies was not convincing enough because of an absence of any additional mechanistic tests,[20c,24a,26] discrepancy in the various test results,[2b,20b,21c,d] and a lack of the expected induction period in the kinetic curve.[9b,20,21a,b,d] The more serious drawback of most of the above-mentioned mechanistic studies (excluding some reports)[9b,24] is the absence of the absolutely necessary control experiments, including the mercury(0) reactions with the starting (pre)catalyst and other catalysis participants; in these circumstances, the mercury drop test interpretation must be recognized as incorrect.[1a,d]

We have proposed that if the alternative Pd(II)/Pd(IV) catalytic cycle for cross-coupling is possible in principle then it may operate either alone or in combination with the classic Pd(II)/Pd(0) route. Previously, we developed a catalytic system with the maximum contribution of the palladacycle-retaining pathway of the Suzuki reaction that is necessary for the efficient chirality transfer in an asymmetric version of this process.[29] The following properties of this system satisfied this condition: The catalyst can operate in air at room and reduced temperatures without any visible evidence of palladium black formation, providing good yields and a rather high enantioselectivity of the binaphthyl product. In addition, the catalyst was almost quantitatively recovered after the reaction completion, and the kinetic curve for this reaction did not reveal any induction period. However, we discovered an unexpected contradiction between these properties of the catalytic system and a positive mercury drop test. The control experiment showed that the reason for the catalysis suppression is the redox-transmetalation of the cyclopalladated (pre)catalyst.[29b] Herein we report an evaluation of the limits of the mercury poisoning test applicability to CPC-catalyzed reactions.

RESULTS AND DISCUSSION

In this research, we worked to solve the following two main problems: to assess the limits of mercury poisoning test applicability for other CPC-catalyzed cross-coupling reactions and to estimate the influence of the control test conditions on the result.

Mercury(0) Testing of Diverse Azapalladacycles. The first problem arose from the fact that the sole known report on palladacycle reactions with mercury(0) was devoted to imine-derived CPCs and aimed at the preparative synthesis of planar chiral ferrocenylmercuric chlorides.[30] Under these circumstances, it was reasonable to assume that the similar anomalous reactivity of high-valent palladium complex **1a** with metallic mercury to provide arylmercuric chloride **1b** (L^1HgCl) as the redox-transmetalation product[29b] is due to the specific properties of the iminate ligand (Scheme 1).

Scheme 1. Redox-Transmetallation of the Catalyst *rac*-1a

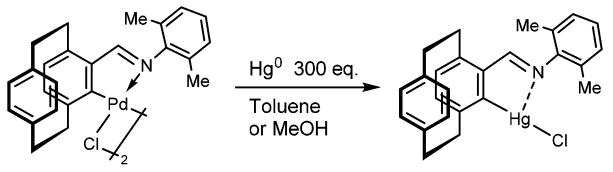

rac-**1a** *rac*-**1b**

To estimate the scope of this unusual reactivity, we performed the main control experiment (required for the classic mercury drop test)[1a,d] for a series of azapalladacycles derived from diverse *N*-donor ligands (Chart 1). This set of potential (pre)catalysts included complexes bearing a tertiary amino-group as an (sp^3)

Chart 1. Structures of the Cyclopalladated Dimers Used in the Present Research

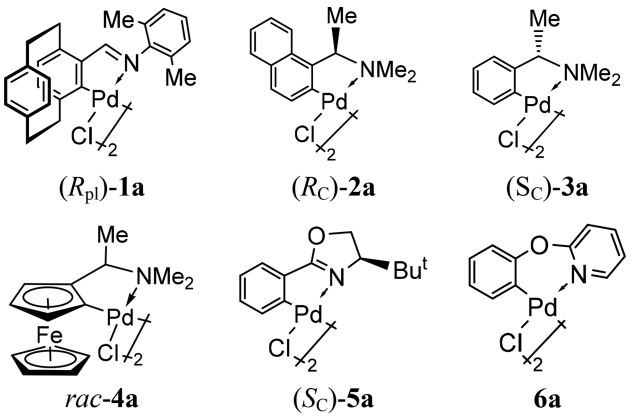

(R_{pl})-**1a** (R_C)-**2a** (S_C)-**3a**

rac-**4a** (S_C)-**5a** **6a**

DOI: 10.1021/acs.organomet.8b00363
Organometallics XXXX, XXX, XXX−XXX

N-donor on an arylene framework (**2a**, **3a**) or a ferrocenylene backbone (**4a**), and two more structures with (sp^2)*N*-donors of oxazolinyl (**5a**) or pyridyl (**6a**) heterocyclic rings in addition to the nonmetallocenic planar chiral iminate *C,N*-dimers (R_{pl})- and *rac*-**1a**. To make the results of such a screening most compelling, all control experiments were conducted on a preparative level, affording the possibility of spectral and structural characterization of the reaction products and mercury(0) of the highest purity (99.999%) was used.

Influence of the Structure and Conditions on the Control Experiment Result. This series of control experiments showed that all *C,N*-palladacycles interact with metallic mercury, affording arylmercuric chlorides (Chart 2), although

Chart 2. Structures of Isolated Organomercuric Chlorides 1b−6b

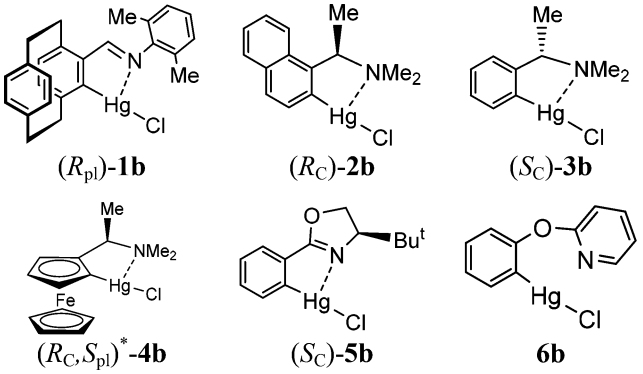

the efficiency of their redox-transmetalation is strongly dependent on the CPC structure and solubility and on the testing conditions (Table 1). All cyclopalladated *C,N*-dimers **1a**−**6a** reacted with metallic mercury in toluene even at room temperature. Under these conditions, the difference in their reactivity was especially pronounced: The yields of isolated arylmercuric chlorides varied from ∼8% after 144 h for **2b** to 71% at 96 h for **5b** (entries 4 and 10, respectively). This process could be considerably accelerated by the introduction of a base: For example, in the presence of potassium fluoride arylmercuric chloride **5b** was isolated after 9 h in a yield of 94% compared to a yield of 71% after 96 h in the absence of base (entries 12 and 10, respectively). The redox-active ferrocenylene backbone of starting dimer **4a** also makes a significant contribution to the acceleration of the transmetalation: After reaction at room temperature for 3.5 h, mercurial **4b** was isolated in a yield of 81%, the yield of its analogue **2b** with a naphthylene backbone and identical side chain was only 8% after 144 h, and starting dimer **2a** was recovered in an intact state in a yield of 61% (entries 8 and 4, respectively).

At increased temperature (up to 70−90 °C), the transformation of *C,N*-CPCs into arylmercuric chlorides was also considerably accelerated. For example, arylmercurials *rac*-**1b**, (S_C)-**5b**, and **6b** were isolated after 1−3 h of heating in yields of more than 90% (entries 2, 11, and 15, respectively), while the same reactions of dimers *rac*-**1a**, (S_C)-**5a**, and **6a** performed at room temperature required 48−96 h (entries 1, 10, and 14, respectively). As one might expect, the low solubility of the starting μ-chloride cyclopalladated dimers makes some contribution to the slowdown of the reaction. For example, the redox-transmetalation of dimer *rac*-**1a**, which is practically insoluble in toluene, required a 3-fold increase in the reaction duration compared to its highly soluble enantiopure form (R_{pl})-**1a** under the same conditions (entries 2 and 3, respectively).

The cross-coupling reactions are usually carried out either under inert gas or in air; therefore, mechanistic testing and diverse control experiments should be conducted strictly in the same atmosphere. As far as we know, estimates of the influence of this factor are extremely rare. They are limited by the mercury poisoning test performance for the phosphite *C,P*-palladacycle-catalyzed Suzuki−Miyaura cross-coupling reaction both in air and under argon with no difference in the results of the first run (90−100% yield of the product)[16a,b] but with controversial results for the second cycle.[16a] Therefore, it was necessary to assess the impact of these conditions on the results of our control experiments. We did not find significant differences in the reactions of *C,N*-dimer (S_C)-**5a** with metallic mercury performed under argon and air: in both conditions redox-transmetalation product (S_C)-**5b** was isolated in almost identical yields (93 and 90%; entries 11 and 12, respectively).

There is one more important factor that determines the rate of the redox-transmetalation process, namely, the mercury(0)-to-palladium(II) ratio. As an illustration of its efficiency, we can compare the results of decreasing the mercury(0) excess from the standard 330 equiv to only 20 equiv in the redox-transmetalation of dimer **5a** at the same temperature: Even after an 8-fold increase in the reaction duration, the yield of arylmercuric chloride **5b** was noticeably reduced (93 and 79%; entries 13 and 11, respectively). It should be noted that in the application of the mercury drop test, this parameter has varied over a very broad range starting from less than 100 equiv of mercury(0)[7b,22,24a] to 4000−20 000 equiv,[14d,19a,21b,d] without any explanation regarding the choice of the value. To emphasize the importance of this factor, we can mention a rare example of its estimation. A drastic dependence of the mercury poisoning effect on the Hg/Pd ratio was reported in Suzuki and Heck reactions (at 110 and 130 °C, respectively) catalyzed by ylide *C,P*-palladacycles: the yield of the cross-coupling product decreased from 73 to 85% in the presence of 100 mercury(0) equivalents down to trace quantities at 300 equiv.[22] From this example, it becomes obvious that the lowering of the mercury(0) excess in the control experiment compared with that used in the mercury poisoning of the catalytic process leads to incorrect conclusions from this kind of mechanistic testing.

Metallic Mercury Reactivity. At first glance, our results from the control experiments may seem anomalous from the standpoint of the widely accepted view on the interaction of metallic mercury with only zero-valent metals[1c,7,9] or (much more rarely) with their molecular complexes.[8] However, there is series of reports (mainly dated in the previous century) that may raise doubts as to the validity of this widespread opinion.

The most powerful argument against this common misconception is provided by the preparative synthesis of a series of cyclomercurated compounds via redox-transmetalation by metallic mercury of chiral azapalladacycles derived from ferrocenylimines under very mild conditions at room temperature. These cyclomercurated compounds were isolated in very high yields (92−98%), exceeding the efficiency of direct cyclomercuration of imine ligands by the standard method. Their structure was convincingly confirmed by elemental analysis, optical rotation values, IR spectral data, and selected ^{1}H NMR spectral data, as well as X-ray crystal structure data and circular dichroism spectral data for one of 12 compounds.[30a] This report by Wu from 1999 remained the sole example of the implementation of the redox-transmetalation of CPCs with

DOI: 10.1021/acs.organomet.8b00363
Organometallics XXXX, XXX, XXX−XXX

Table 1. Mercury(0) Poisoning of Diverse Palladacycles (Control Experiments)[a]

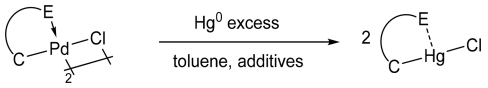

Entry	Starting dimers	Hg(0) excess (equiv./Pd)	Temperature, °C	Duration, hrs	Yield [b], %	Reaction product
1 [c]	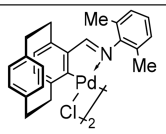	300	r.t.	48	60	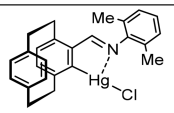
2 [c]		330	110	3	90	
3 [d]		300	90	1	90	
	rac-**1a**					(R_{pl})*-**1b**
4	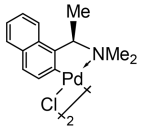	330	r.t.	144	7.8 [e]	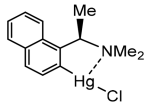
5 [f]		330	70	9	81	
	(R_C)-**2a**					(R_C)-**2b**
6 [f]	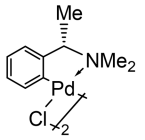	330	r.t.	96	55	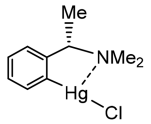
7		330	70	8	78	
	(S_C)-**3a**					(S_C)-**3b**
8 [f]	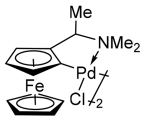	298	r.t.	3.5	81[g]	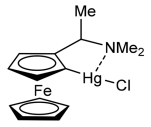
9 [f]		330	70	1	60	
	rac-**4a**					*rac*-**4b**
10 [f]	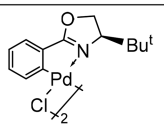	330	r.t.	96	71	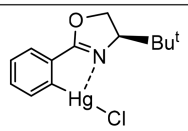
11 [f]		330	70	1	93	
12		330	70	1	90	
12 [f,h]		330	r.t.	9	94	
13		20	70	8	79	
	(S_C)-**5a**					(S_C)-**5b**
14	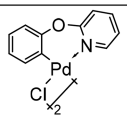	330	r.t.	96	22	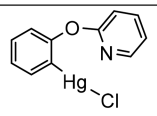
15		330	70	1	92	
	6a					**6b**

[a]Typical reaction conditions: mixture of the cyclopalladated dimer (~0.05 mmol) and metallic mercury excess (~33 mmol, 330 equiv) was intensively stirred in toluene (~15 mL) under air (if not stated otherwise). [b]Isolated yield is presented. [c]Experiments were conducted with a racemic cyclopalladated dimer of extremely low solubility. [d]The enantiopure dimer (R_{pl})-**1a** was completely soluble in toluene, in contrast to the insoluble racemic form. [e]Starting cyclopalladated dimer was recovered in a yield of 61%. [f]The reaction was performed under argon. [g]Yield of pure complex **4b** (TLC and ^{1}H NMR data) isolated as red-brown oil; after multistage crystallization, one of its racemic diastereomers was separated in a yield of 53% in the crystal state. [h]The reaction was conducted in the presence of KF (10 equiv/Pd).

mercury(0) published before the beginning of our own research.[29b] Before the report by Wu, the similar Pd^{II}/Hg^0 redox-exchange was realized with a nontypical analogue of CPCs, $[\{(\eta^2,\eta^1C,C,C\text{-L})Pd(\mu\text{-Cl})\}_2]$ (L^- = acetoxynorbornenyl), affording the alkylmercuric chloride $[(\eta^1C\text{-L})HgCl]$ in a yield of 30%.[31] In addition, we can mention the related redox-transmetalation processes, namely, interaction of planar chiral cyclopalladated ferrocenylimines (as μ-chloride dimers) with zero-valent tin to afford cyclometalated Sn(IV) derivatives (S_{pl},S_{pl})-$[(\kappa^2C,N\text{-L})_2SnCl_2]$.[32]

As another valuable contribution to disproving the common misconceptions regarding limited mercury(0) reactivity, we can mention the Nesmeyanov's research devoted to the investigation of mercury(0) reactions with diverse π-allyl palladium(II) complexes.[33] It was shown that these reactions provide allylmercuric halides or bis(allyl)mercurials (along with metallic palladium) in high yields under mild conditions. As a rare exception to this high reactivity, we can mention that the triphenylphosphine derivative $[(\eta^3\text{-All})PdCl(PPh_3)]$ of the allylic μ-chloride dimer was found not to react with metallic mercury.[33c] The authors proposed a mechanism for this reaction, including the cleavage of the μ-halide bridges in the π–AllPdCl molecule, π–σ-rearrangement of the π-allyl ligand, causing cis-migration of the σ-bonded allyl group from palladium to the mercury atom, and final internal redox reaction producing palladium(0) and alkylmercury chloride.[33c]

DOI: 10.1021/acs.organomet.8b00363
Organometallics XXXX, XXX, XXX–XXX

Moreover, efficient mercury(0) interactions with palladium(II) compounds have even found analytical applications.[34] Several examples from platinum(II) chemistry may also be mentioned. First, it was shown that high-temperature thermolysis of organometallic platinum(II) complex $R_2Pt(cod)$ (R = $^tBuCH_2$, cod = cycloocta-1,5-diene) in the presence of mercury(0) results in the formation of dialkyl mercurial HgR_2 in high yield.[35] Second, complete poisoning of high-valent platinum catalysts, $(cod)Pt^{II}Cl_2$ and even $H_2Pt^{IV}Cl_6$ (Speier's catalyst), was observed after their long treatment with mercury(0) before introduction of the other reaction participants.[8a,36] Among the other redox processes on a mercury(0) surface we can also mention the formation of R_2Hg mercurials (R = aryl, alkyl) from thallium(III) organometallic compounds, TlR_3 or R_2TlHlg.[37]

Consequences for Catalysis Studies. Therefore, mercury(0) reactions with homogeneous molecular metal complexes in elevated formal oxidation states cannot be considered exotic precedents. Thus, in the case of a positive mercury drop test it is absolutely necessary to perform additional control experiments to ensure that the (pre)catalyst does not react with mercury(0) under the catalysis conditions.[1a,b,38] However, to the best of our knowledge, among the many dozens of publications on the use of the mercury poisoning test for mechanistic elucidation of CPC-catalyzed reactions, only three examples of such control experiment performance are known. All these probes were made for catalytic systems with pincer (pre)catalysts and using only NMR control.[9b,24] Thus, it was shown that phosphinite *P,C,P*-pincer palladium(II) complexes do not react with mercury(0) alone but undergo oxidation and probably hydrolysis in the presence of a mercury(0) and Cs_2CO_3 mixture. This assumption was based on the observed similarity of the $^{31}P\{^1H\}$ NMR chemical shifts with those for known phosphine oxide $^iPr_2PhP(=O)$ and phosphinate $^iPr_2P(=O)OPh$.[24]

The third version of the reported control experiment[9b] seems rather inconclusive. First, it was performed in the presence of too low of a mercury(0) excess, namely, with only 20 equiv compared with the 300−500 equiv used in this work for the mercury poisoning of catalysis. Second (and most importantly), the assumption of the intact state of the neutral $[(\kappa^3S,C,S\text{-}L)PdCl]$ pincer (pre)catalyst in the presence of mercury(0) was based on ^1H NMR spectral data confirming the retention of the pyridine (Py) coordination with palladium in the case of the cationic derivative $[(\kappa^3S,C,S\text{-}L)Pd(Py)]BF_4$, which was not used either in the Heck coupling catalysis or in the mercury(0) poisoning test. This probe cannot be recognized as a correct control experiment, taking into account the known drastic difference between the behavior in catalysis of the neutral pincer (pre)catalyst $[(\kappa^3C,N,O\text{-}L')PdI(\kappa^2CO\text{-}L'')]$ and its cationic dehalogenated derivative and the opposite results obtained from the mercury(0) poisoning test for these species.[14c,d]

A positive mercury poisoning test was reported for almost all cross-coupling reactions catalyzed by *C,N*-palladacycles.[21a−f] This result was used as the basis for the assumption of the leading role of palladium(0) NPs, colloidal or low-ligated palladium(0) species in the catalytic processes. Since these studies did not include any control experiments excluding the possibility of (pre)catalyst deactivation due to its reaction with mercury(0), an alternative explanation for the positive mercury poisoning test must be discussed. Several arguments can be made in favor of possible (pre)catalyst killing by mercury(0). First, the close structural similarity of azapalladacycles bearing tertiary amino groups,[21b−f] pyridine,[21a] or an oxazoline *N*-donor,[20c] with our CPCs **2a**−**6a** tested in the control experiments (Table 1) allows us to assume a similar reactivity of these palladacycles with mercury(0). Second, the high temperature regime used for the mercury drop test in Suzuki−Miyaura and Mizoroki−Heck reactions (from 80 to 140 °C) should significantly speed up the redox-transmetalation process. Third, inhibition of catalysis at the introduction of mercury(0) at the starting point of the reaction[21a−c] can serve as evidence for the interaction of Hg(0) with the (pre)catalyst and not with the product of its activation. Fourth, the lack of the expected induction period in the kinetic curve[20c,21a,b,d] and some contradictions between the mercury poisoning and other testing results[21c,d] are also important evidence of the alternative interpretation of the positive mercury test. Finally, all these facts indicate that the most likely reason for the positive mercury(0) poisoning test may be the redox-transmetalation of the palladium(II)-containing *C,N*-metallacyclic (pre)catalyst, not the suppression of catalysis via Pd(0)/Hg(0) interaction. The authors can confirm or refute the alternative explanation of this test result with a simple control experiment.

Confirmation of the Structure of the Redox-Transmetalation Products. The next task of our research was to provide the most convincing evidence of the structure of organomercuric chlorides **1b**−**6b** because (i) they were isolated under unusual circumstances and (ii) they are mainly new compounds. Among mercurials **1b**−**6b**, (S_C)-**3b**,[39] and *rac*-**4b**[40] were previously prepared by classic routes based on the interaction of mercury(II) chloride with the corresponding metalated ligand: (S_C)-L^3Cu,[39b] (S_C)-L^3Li,[39a] or *rac*-L^4Li.[40] To solve our structural problem, we used ^1H, $^{13}C\{^1H\}$, and $^{199}Hg\{^1H\}$ NMR spectroscopy, X-ray diffraction analysis of four mercurials, and density functional theory (DFT) calculations.

Crystal Structure of Mercurials. The X-ray diffraction study of arylmercurial *rac*-**1b** was reported previously without a discussion of its structure;[29b] in this work we performed a crystallographic study of other organomercuric chlorides (R_C)-**2b**, (R_CS_{pl})*-**4b**, (S_C)-**5b**, and **6b** (Table 2, Figures S41−S44) isolated in our control experiments. Among these complexes, only a derivative of the tertiary α-methylbenzylamine, (S_C)-**3b**, had been previously crystallographically characterized.[39a] With the exception of the arylmercuric chloride (R_C)-**2b**, all remaining complexes have only one or no close enough analogues in the rich collection of related mercurials (Tables S1−S6); therefore, for their structure discussion we were forced to use more distant analogues (Chart 3).

The interpretation of the X-ray diffraction data obtained in the previous century sometimes needs to be significantly adjusted by taking into account the modern revision of the van der Waals radii (R_{vdW}): Instead of the previously widely accepted Bondi value of 1.55 Å for the mercury atom,[41] the recently recommended values are 1.73−2.00 Å[42] (corresponding to the *ab initio*-calculated R_{vdW} value equal to 1.75 Å)[43] or 2.1−2.2 Å.[44] Taking into account the recommended crystallographic van der Waals radii of mercury and nitrogen (2.00 and 1.6 Å, respectively),[44a] we can see that the Hg−N distances observed in the structures of isolated organomercurials **1b**, **2b**, **4b**, and **5b** (2.59−2.82 Å) are essentially shortened in comparison with the sum of their van der Waals radii (3.6 Å), even after their correction based on packing effects (~0.2 Å).[45] These parameters allow us to propose the formation of optimal five-membered mercuracycles in the crystals of **1b**, **2b**, **4b**, and **5b**.

DOI: 10.1021/acs.organomet.8b00363
Organometallics XXXX, XXX, XXX−XXX

Table 2. Comparison of the Structural and Stereochemical Characteristics of Isolated Mercurials 1b−6b with Those of Their Analogues[a]

Structures → Parameters ↓	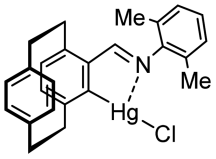	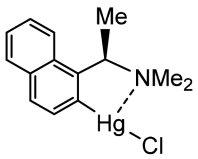	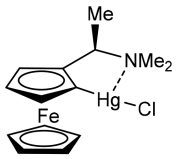	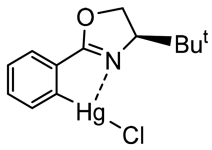	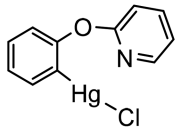
codes	*rac*-**1b**, *anti*-D_{Cl}	(R_C)-**2b**, M	(R_CS_{pl})*-**4b**, *anti*-D_{Cl}	(S_C)-**5b**	**6b**, *anti*-D_{Cl}
Hg···N, Å	2.586 (2.69-2.90)	2.620 (2.65-2.76) [d]	2.824 (4.03-4.27)	2.657 (2.61-2.94)	3.253 [b], 3.004 [c] – [e]
Hg–C^1, Å	2.076 (2.01-2.07)	2.089 (2.04-2.07) [d]	2.078 (2.04-2.06)	2.046 (2.01-2.08)	2.072 – [e]
Hg–Cl, Å	2.343 (2.30-2.31)	2.340 (2.32-2.33) [d]	2.364 (2.32-2.35)	2.326 (2.29-2.31)	2.338 – [e]
Hg–Cl′, Å	3.209 [f] –	–	3.195 [f] (3.22-3.27)	3.187, 3.535 [g]	3.292 [h] – [e]
∠C^1-Hg-Cl, °	179.11 (169.8-179.0)	178.79 (174.2-176.9)	171.08 (164.2-177.9)	175.33 (174.8-176.1)	173.50 – [e]
∠C^1-Hg-N, °	76.64 (71.0-74.0)	76.23 (74.1-75.0)	73.85 (54.7-100.4)	75.34 (70.4-75.2)	67.06 – [e]
ω_{env}, ° [i]	2.41 (2.4-17.4)	42.41 (41.1-47.0) [j]	43.24 –	9.77 (0.0-9.2)	–
ϖ_{av}, ° [k]	1.60 (1.9-11.6)	29.02 (26.8-30.2) [j]	30.68 –	6.69 (0.0-7.5)	– [e]

[a]The ranges of the same parameters for related compounds are presented in round brackets (see the Supporting Information). [b]Intramolecular distance Hg···N. [c]Intermolecular distance Hg···N′. [d]Data only for known related arylmercuric chlorides (Table S3). [e]Analogues are unknown. [f]Intermolecular Hg−Cl′ contacts in the plane approximately orthogonal to the mercuracycle. [g]The organomercury chloride crystallizes in the form of an infinite chain of mutually orthogonal dimers connected by stronger chloride bridges in the axial position and weaker equatorial bridges. [h]Intermolecular Hg−Cl′ contacts nearly in the plane of the mercuracycle. [i]The interplanar angle {$HgNC^{\alpha}$}/{$HgC^1C^2C^{\alpha}$} denoted as ω_{env} was used for characterizing the mercuracycle envelope-shaped bending. [j]Data for all known related arylmercuric halides (Table S3). [k]Mercuracycle twisting, ϖ_{av}, is calculated as the average of the absolute values of all intrachelate torsion angles.

In general, all structures of these isolated organomercuric chlorides may be considered typical representatives of the corresponding organomercurials.[45,46] In accordance with the preferable sp-hybridization of mercury(II), they contain an almost linear C−Hg−Cl segment, with the corresponding angles varying over a rather narrow range 171.8−179.1° (Table 2). Their other geometric characteristics, such as the Hg−C, Hg−N, and Hg−Cl bond lengths, and valent angles either fall into the intervals of the values for their known analogues or lie close to the boundaries of these intervals (Tables S1−S6). The geometric parameters of all five-membered mercuracycles are similar to those of their nearest analogues. In derivatives of tertiary amines (**2b**, **4b**), mercuracycles are highly puckered in the envelope-like conformation, with the parameter ϖ_{av} (average of the absolute values of all intrachelate torsion angles) equal to 29.0−30.7° and an interplanar angle {$HgNC^{\alpha}$}/{$HgC^1C^2C^{\alpha}$} (ω_{env}) of 42.4−43.2° (Table 2). In contrast, the mercurials with (sp^2)-hybridized *N*-donors (**1b**, **5b**) contain an almost flat mercuracycle, with ϖ_{av} and ω_{env} values varying in the ranges 1.6−6.9 and 2.4−9.9°, respectively. It should be noted that there are a few main distinctive structural and stereochemical features of our new mercurials.

Surprising, among the extensive collection of mercurated arylimines in the Cambridge Crystallographic Data Centre (CCDC), we have not found close enough analogues (not only stereochemical but also structural analogues) to the non-metallocenic planar chiral organomercuric chloride *rac*-**1b**. As a result, for its geometric parameters analysis, we were forced to use the simplest achiral analogues, namely, the bromide[47] and azides[48] of mercurated *N*-arylbenzaldimines (**A**) and related planar chiral organomercuric chlorides derived from *N*-arylferrocenylaldimines or -ketimines (**B**)[49] (Table S2). In the complex *rac*-**1b**, the Hg−C and Hg−Cl bonds are somewhat elongated in comparison with models **A** and **B**, while the Hg−N

DOI: 10.1021/acs.organomet.8b00363
Organometallics XXXX, XXX, XXX−XXX

Chart 3. Generalized Structures of Models A–F

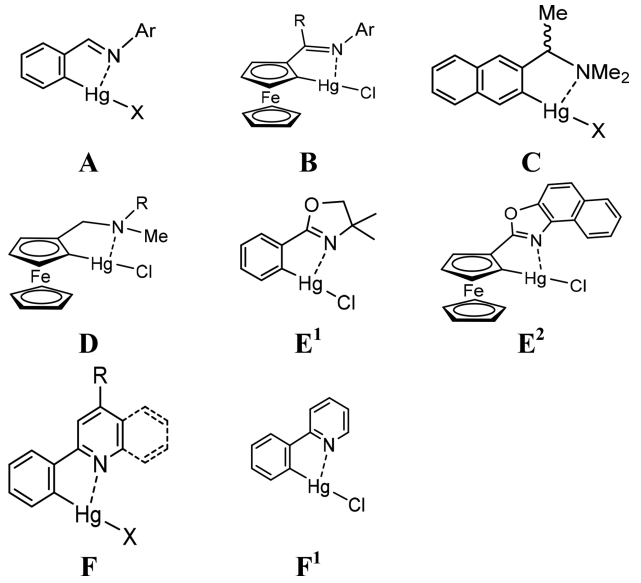

bond in compound **1b** is noticeably stronger than that in analogues **A** and **B**. Racemic mercurial **1b** exists in the crystal as a chloride-bridged dimer containing both (R_{pl})- and (S_{pl})-enantiomers, with the central four-membered core {Hg(μ-Cl)$_2$Hg} oriented nearly orthogonally between two approximately parallel mercuracycles with an interplanar angle {Hg$_2$Cl$_2$}{C^{1}C^{2}C$^\alpha$NHg} equal to 82.45° (Figure 1). It should

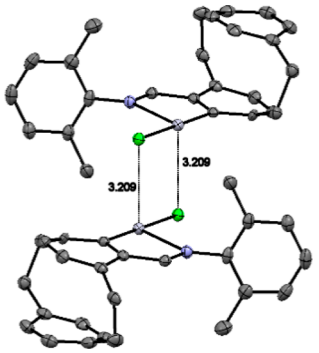

Figure 1. Fragment of the crystal packing of mercurial *rac*-**1b** showing the dimerization via two intermolecular Hg···Cl′ bridges in the approximately axial position.

be noted that intermolecular Hg···Hlg′ interactions are not found in model bromide **A** (Ar = Ph, X = Br) and chlorides of type **B**. In the dimer *rac*-**1b**, the *N*-aryl ring is rotated relative to the mercuracycle to 73.3°, while the corresponding angles vary widely from 2.4 to 88.1° in model structures **A** and **B**.

The *C*,*N*-mercuracycle in compound (R_C)-**2b** with a naphthylene-1,2 backbone is fixed in the crystal in the δ(R_C) conformation with an axial position of the Me group at the α-carbon stereocenter, which is evident from the torsion angle C^{1}C^{2}C$^\alpha$C(Me) equal to −82.7° (Figure 2). In contrast, the known analogues of type **C** with phenylene[39a] or naphthylene-2,3[50] backbones contain the similar mercuracycle in the λ(R_C) or δ(S_C) conformation with an equatorial orientation of the α-methyl group, which is evident from the variation of the absolute value of the same angle C^{1}C^{2}C$^\alpha$C(Me) varied in the range 166.2–174.2° (Table S3). This contrasting stereochemistry is

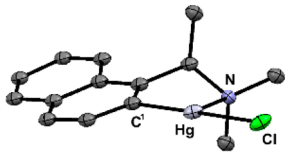

Figure 2. Molecular structures of the organomercuric chloride (R_C)-**2b**. Hydrogen atoms are omitted for clarity, and only selected atoms are labeled. Thermal ellipsoids are given at 50% probability level.

similar to that reported for the corresponding *C*,*N*-palladacycles.[51] As an additional peculiarity of the mercurial (R_C)-**2b**, we can note that it exists in the crystal as a monomer, in contrast to the extensive systems of intermolecular Hg···Cl secondary interactions typical for its analogues of type **C** (Chart 3).

The most amazing feature of ferrocenylmercuric chloride **4b** is its chelated structure with an intramolecular Hg–N bond of 2.82 Å (Table 2, Figure 3a), which is closer to the sum of the

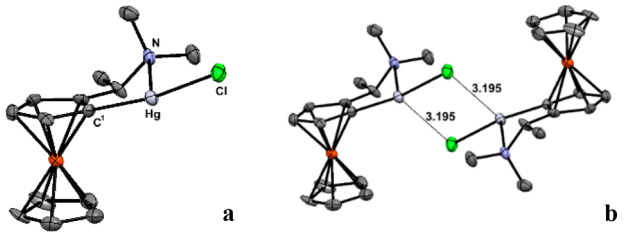

Figure 3. Molecular structure of the organomercuric chloride (R_C,S_{pl})*-**4b** (a). Formation of an *anti*-dimeric structure in the crystal for ferrocenylethylamine mercurial (R_C,S_{pl})*-**4b** via the weak intermolecular interactions Hg···Cl (b). Hydrogen atoms are omitted for clarity, and only selected atoms are labeled. Thermal ellipsoids are given at 50% probability level.

covalent radii of these atoms[52] than to the sum of their van der Waals radii (2.34 and 3.65 Å, respectively). In contrast, mercuracycles were not detected among the related derivatives of α-nonsubstituted tertiary ferrocenylmethyl amines (type **D**), in which the intramolecular Hg···N distances are larger than 4.0 Å[53] (Table S4). According to the negative or positive signs of the C^{1}C^{2}C$^\alpha$N torsion angle in the isolated racemic mixture of ($R_C$$S_{pl}$)- and ($S_C$$R_{pl}$)-diastereomers of mercurial **4b** (−50.22 or 50.22°, respectively), the mercuracycle conformation in them must be described as λ(R_C) or δ(S_C), respectively, with an equatorial position of the α-methyl group in both diastereomers, which is evident from the torsion angle C^{1}C^{2}C$^\alpha$C(Me) equal to −179.1°. These conformational peculiarities most likely define the dimerization of organomercuric chloride ($R_C$$S_{pl}$)*-**4b** via two chloride bridges, with a central four-membered fragment {Hg(μ-Cl)$_2$Hg} oriented nearly orthogonally between two approximately parallel mean coordination planes (Figure 3b). For comparison, similar α-nonsubstituted ferrocenylmethylamines in known mercurials **D** prefer to function mainly as *C*,*N*-bridging ligands at rather short intermolecular Hg···N′ distances (2.77–2.93 Å). In addition, the metal participates in the secondary intermolecular Hg···Cl′ interactions oriented intermediately between the axial and equatorial positions with torsion angles ∠Cl′HgC^{1}C^2 reduced by 32–45° compared to 180° (Table S4).

We can note two differences of mercurial (S_C)-**5b** bearing a chiral oxazolinyl *N*-donor from its closest achiral analogue (**E^1**)[54] and from the less similar organomercuric chloride derived from the 2-ferrocenylnaphthoxazole (**E^2**)[55] (Chart 3,

DOI: 10.1021/acs.organomet.8b00363
Organometallics XXXX, XXX, XXX–XXX

Table S5). First, our complex (S_C)-**5b** crystallizes as infinite double-folded tapes consisting of mutually orthogonal dimers connected by stronger chloride bridges in the axial position and weaker equatorial chloride bridges at Hg···Cl′ and Hg′···Cl distances equal to 3.187 and 3.535 Å, respectively (Figure 4).

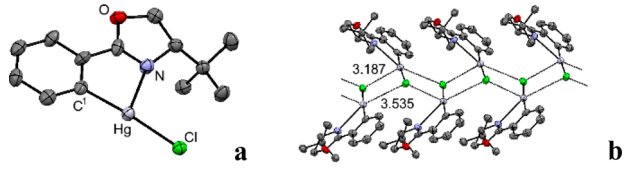

Figure 4. Molecular structure of organomercuric chloride (S_C)-**5b** (a). Fragment of the crystal packing of mercurial (S_C)-**5b** illustrating the formation of infinite double folded tapes via intermolecular chloride bridges between the mutually orthogonal dimers with stronger Hg···Cl′ interactions in the axial position than in the equatorial position at distances equal to 3.187 and 3.535 Å, respectively (b). Hydrogen atoms are omitted for clarity, and only selected atoms are labeled. Thermal ellipsoids are given at 50% probability level.

Conversely, intermolecular secondary interactions of this kind were not found in the crystal of its achiral analogue **E**[1], and only one axial chloride bridge between two nonequivalent organomercuric chlorides at a distance of 3.245 Å was observed in the case of 2-ferrocenylnaphthoxazole derivative **E**[2]. Second, the mercuracycle of complex (S_C)-**5b** possesses puckering similar to that found for its naphthoxazole analogue **E**[2], in contrast with the ideally planar metallacycle in oxazoline analogue **E**[1] with ϖ_{av} values equal to 6.9, 7.5−5.2, and 0.0, respectively, despite the comparable Hg−N bond lengths in the first two compounds.

The only exception in our series of mercurated compounds is arylmercurial **6b** with an intramolecular Hg···N distance elongated up to 3.27 Å but containing a shorter intermolecular Hg···N′ contact of 3.004 Å (Figure 5, Table S1). Its structure is

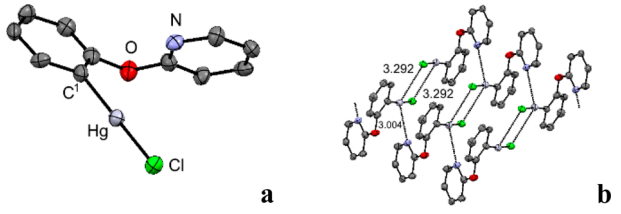

Figure 5. Molecular structure of the organomercuric chloride **6b** (**a**). A fragment of the crystal packing of the arylmercury chloride **6b** showing rather short intermolecular contacts Hg···N between the chains of nearly parallel dimers formed due to intermolecular Hg···Cl bridges in the mean coordination plane (**b**). Hydrogen atoms are omitted for clarity, and only selected atoms are labeled. Thermal ellipsoids are given at 50% probability level.

composed of chloride-bridged dimers formed due to the intermolecular Hg···Cl′ contacts at a distance of 3.292 Å, which is less than the sum of the van der Waals radii of these atoms (3.85 Å).[44a] An unusual property of this structure is the anomalous, almost coplanar disposition of the central four-membered core {Hg(μ-Cl)$_2$Hg} relative to the phenylmercuric fragment, with the interplanar {Hg_2Cl_2}{PhHgCl} angle equal to 8.77° (Figure 5). The pyridine rings of these dimers are rotated relative to the phenylmercuric chloride mean plane by 60.98° to connect the adjacent parallel columns of dimers via intermolecular Hg···N′ contacts at a distance of 3.004 Å. Thus, arylmercurial **6b** structure is typical of mercury(II) compounds, which prefer Hg···N′ intermolecular interactions rather than *C,N*-chelation if the latter leads to the formation of a six-membered metallacycle. It should be noted that the CCDC does not contain any data for organomercurials with six-membered *C,N*-mercuracycles. However, coordination compounds with six-membered *N,N*-chelate rings formed by diamine[56] or diimine ligands[57] are known. In contrast to the T-shaped functionalized organomercuric chlorides, they contain the (sp^3)-hybridized mercury(II) atom in a distorted tetrahedral coordination environment with a rather strong Hg−N bonds (2.246−2.475 Å) inside the chair-shaped chelate ring. In contrast to T-shaped functionalized organomercuric chlorides, these chelates contain the (sp^3)-hybridized mercury(II) atom in a distorted tetrahedral coordination environment with rather strong Hg−N bonds (2.246−2.475 Å) inside the chair-shaped chelate ring.

DFT Calculations of Organomercurials. To estimate the possibility of formation of six-membered *C,N*-mercuracycles and to exclude the effect of crystal packing, we performed DFT calculations and geometry optimization for arylmercury(II) chloride **6b** and its chelated model with a five-membered mercuracycle (κ^2*C,N*-**F**[1]) in the gas phase. The two most important differences between the experimental and calculated structures should be noted (Figure 6, Table S12): the rotation of

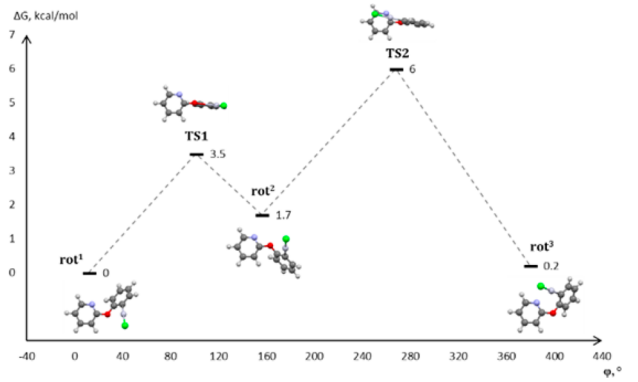

Figure 6. Energy profile of the rotation of mercurial **6b** about the (Py)C$^{2'}$−O bond.

the pyridyl ring from the nearly coplanar position in the crystal ca. 20° of the optimized structure (**rot**[3]) with torsion angles C^{2}OC$^{2'}$N equal to 4.0 and −19.67°, respectively, and a shortening of the intramolecular Hg···N distance from 3.253 Å in the crystal to 2.915 Å in the gas phase. The last value is close to the upper limits of the characteristic ranges typical for five-membered *C,N*-mercuracycles bearing (sp^2)-hybridized nitrogen donors: 2.69−2.90 Å for iminoaryl derivatives (Table S2) or 2.60−2.80 Å for pyridyl-donor analogues (Table S6). The observed evidence of weak intramolecular Hg···N interactions calculated for the gas phase structure of mercurial **6b** may be explained by excluding under these conditions any competing intermolecular interactions such as Hg···N′ and Hg···Cl′, which were detected in the crystal state.

The rotation of the pyridine ring about the C$^{2'}$−O bond of the 2-phenoxy-pyridine ligand of mercurial **6b** revealed three possible rotamers (**rot**[1]−**rot**[3]) formed via transition states **TS1** and **TS2** with barriers of 3.5 and 6.0 kcal/mol respectively (Figure 6). The parameters of rotamer **rot**[3] correspond to its chelated form with a very weak intramolecular Hg···N interaction (bond order, 0.14). However, despite intermediate

DOI: 10.1021/acs.organomet.8b00363
Organometallics XXXX, XXX, XXX−XXX

rotamer **rot**^{2} having higher energy (ΔG 1.7 kcal/mol) than rotamer **rot**^{3}, the most stable form was dechelated rotamer **rot**^{1} with an energy of only 0.2 kcal/mol lower than that of the *C,N*-chelated mercurial.

The nature of the secondary Hg···N intramolecular interaction in the mercurial **6b** was estimated using Bader's atoms-in-molecule (AIM) theory.[58] The topological analysis of electron density at the Hg···N bond (Figure 7a) revealed the bond critical point (bcp) with the following parameters: a low total electron density $\rho(r_c)$ at the bcp (0.02 au), low positive value of Laplacian $\nabla^2\rho(r_c)$ (0.06 au), and ratio of the perpendicular contractions of ρ to its parallel expansion, $|\lambda_1\backslash\lambda_3|$ (0.16). These topological properties indicate the formation of an extremely weak noncovalent bond or closed-shell interaction.

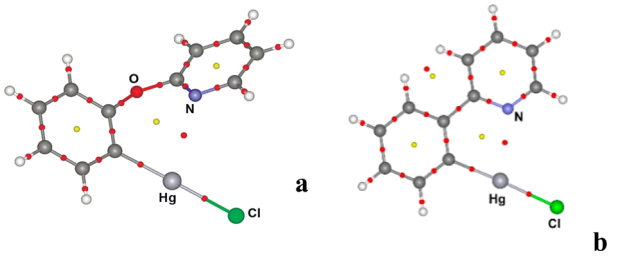

Figure 7. Bond (red) and cycle (yellow) critical points for the six-membered mercuracycle **6b** (a) and its five-membered analogue **F**^{1} (b) according to topological analysis in AIM theory.

To estimate the influence of the chelate ring size on the mercurial stability, we also performed similar DFT calculations for the known analogue **F**^{1} (L′HgCl) derived from 2-phenylpyridine (HL′) and bearing a five-membered mercuracycle.[59] Its optimized structure (Table S13) contains a stronger Hg−N bond (2.661 Å) of higher order (0.23). The rotation of the pyridyl ring about the single $C^2-C^{2'}$ bond reveals the higher stability of the *C,N*-chelated form **rot**$^{1'}$ compared to dechelated rotamers **rot**$^{2'}$ and **rot**$^{3'}$ (5.4 kcal/mol) with rotation barriers of 9.0−9.5 kcal/mol (Figure S40). The enantiomeric nature of these helical rotamers is evident from the opposite signs of the torsion angle $NC^{2'}C^2C^1$, equal to −139.02 and +139.09° in **rot**$^{2'}$ and **rot**$^{3'}$, respectively. The topological analysis of the optimized **F**^{1} structure (Figure 7b) provides the following parameters for the Hg−N bcp: slightly higher total electron density $\rho(r_c)$ at the bcp (0.03 au), increased values of the Laplacian $\nabla^2\rho(r_c)$ (0.11 au), and a $|\lambda_1\backslash\lambda_3|$ ratio of 0.18. These parameter values indicate a slightly higher stability of the Hg−N bond in the five-membered mercuracycle of the model mercurial **F**^{1} compared to its six-membered counterpart **6b**.

Unfortunately, DFT calculations of mercurated nitrogen donors are very limited,[47,48,60] and only two reports were devoted to the mercurials bearing (sp^2)-hybridized nitrogen donors.[47,48] It was shown that the secondary Hg···N intramolecular interaction energy of the mercurated benzaldimine bromides L′HgBr (**A**^{1}) is on the order of 2.5−3 kcal/mol.[47] An energy difference of 6.4 kcal/mol was found between the chelated and dechelated rotamers of azidomercurated benzaldimine L′HgN$_3$. The topological parameters $\rho(r_c)$ and Laplacian

Table 3. ^{199}Hg{^{1}H}, ^{1}H and ^{13}C{^{1}H} NMR Spectral Parameters of Organomercuric Chlorides 1b−6b[a]

Structures → Parameters ↓	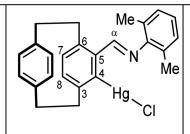	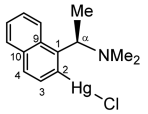	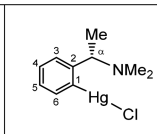	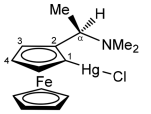	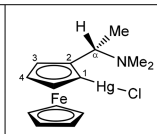	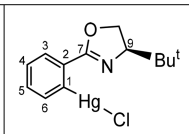	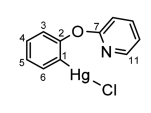
code	(*R*$_{pl}$)-**1b**	(*R*$_C$)-**2b**	(*S*$_C$)-**3b**	(*R*$_C$,*S*$_{pl}$)*-**4b**	(*S*$_C$,*S*$_{pl}$)*-**4b** [b]	(*S*$_C$)-**5b**	**6b**
δ_{Hg}, ppm	-978	-905	-933	-734	-685	-1057	-1115
^{1}H NMR: δ_H, ppm ($^nJ_{HHg}$, Hz)							
H^3			7.22 (–)	4.36 (^4J = 31)	4.12 (–)	7.88 (^4J = 62)	7.15 (–)
H^4	6.57 (–) for H^7		7.23 (–)	4.22 (^4J = 42)	4.33 (–)	7.35 (^5J = 17)	7.36 (–)
H^5	6.63 (^4J = 78) for H^8	7.72 (^4J = 54) for H^4	7.22 (–)	4.06 (^3J = 51)	4.12 (–)	7.51 (^4J = 49.4)	7.23 (–)
H^6		7.56 (^3J = 187) for H^3	7.41 (^3J = 223)			7.41 (^3J = 206)	7.35 (^3J = 208)
H$^\alpha$	8.63 (^4J = 10)	4.48 (–)	3.51 (–)	3.92 (–)	3.26 (–)		
^{13}C{^{1}H} NMR: δ_C, ppm ($^nJ_{CHg}$, Hz)							
C^1	153.80 (–) for C^4	145.01 (^1J = 2495) for C^2	147.04 (^1J = 2464)	87.14 (–)	81.92 (–)	150.62 (^1J = 2567)	142.59 (^1J = 2378)
C^2	138.11 (^2J = 48) for C^5	147.09 (^2J = 51) for C^1	150.73 (^2J = 49)	95.14 (^2J = 131)	98.40 (–)	167.76 (^2J = 105)	157.06 (^2J = 30)
C^3	144.04 (^3J = 164) for C^6	131.56 (^3J = 194) for C^9	128.50 (^3J = 169)	72.27 (^3J = 253)	71.62 (^3J = 260)	128.54 (^3J = 145)	121.50 (^3J = 104)
C^4	136.11 (^4J = 30) for C^7	133.78 (–) for C^{10}	128.81 (^4J = 31)	69.07 (^3J = 206)	70.13 (^3J = 208)	128.54 (^4J = 29)	130.48 (^4J = 19)
C^5	135.93 (^3J = 202) for C^8	126.93 (^3J = 208) for C^4	127.32 (^3J = 214)	67.86 (^2J = 156)	66.17 (^2J = 160)	132.21 (^3J = 209)	125.38 (^3J = 193)
C^6	146.36 (^2J = 91) for C^3	133.69 (^2J = 134) for C^3	137.32 (^2J = 140)			136.96 (^2J = 132)	136.65 (^2J = 78)
C$^\alpha$	161.96 (^3J = 118)	60.97 (^3J = 106)	66.05 (^3J = 93)	59.81 (^3J = 34)	56.00 (^3J = 26)	132.14 (^3J = 40) for C^7	163.07 for C^7
(C$^\alpha$–N)–**C**	149.42 (–) for N-C^{ipso}	42.3; 44.2 (–)	42.52 (–)	39.19 (–)	41.21 (–)	75.54 (^3J = 14) for C^9	147.56 (–) for C^{11}

[a]Numbering scheme for complexes **3b**−**6b**: The carbon directly connected to mercury is first, with increasing carbon numbers in the direction of a substituent. However, for mercurials (*R*$_{pl}$)-**1b** and (*R*$_C$)-**2b** possessing ligands with established numbering conventions, such conventions were maintained. [b]The minor diastereomer parameters were extracted from the spectra of a mixture of both diastereomers.

DOI: 10.1021/acs.organomet.8b00363
Organometallics XXXX, XXX, XXX−XXX

$\nabla^2\rho(r_c)$ of the iminate five-membered mercuracycle were equal to 0.026 au and 0.027 au, respectively.[48]

Structure of the Organomercuric Chlorides in Solution. The structure and stereochemistry of arylmercuric chlorides **1b**−**6b** isolated in our control experiments were confirmed by ^{1}H, ^{13}C{^{1}H}, and ^{199}Hg{^{1}H} NMR spectroscopy, with signal assignments based on the gCOSY, gHMQC, and gHMBC techniques. It should be noted that the NMR spectral studies were reported only for mercurial (S_C)-**3b**,[39] while its ferrocenyl analogue *rac*-**4b** was characterized only by elemental analysis.[40] We succeeded in the isolation of one of its two racemic diastereomers, namely, the major one, (R_CS_{pl})*-**4b**; the relative configurations of the α-carbon center and planar chirality were established by X-ray diffraction analysis of this predominant diastereomer (*vide supra*).

The spectral data for organomercuric chlorides **1b**−**6b** are in agreement with the recognized trends in the NMR characteristics of this class of mercurials,[46d,61] which confirms their structure. The ^{199}Hg NMR chemical shifts for arylmercuric chlorides **1b**−**3b**, **5b**, and **6b** were observed from −905 to −1115 ppm, while a highfield shift to −685 or −734 ppm was found for diastereomeric ferrocenylmercuric chloride **4b** (Table 3). These values are close to the previously reported values for related organomercury chlorides (Tables S7−S11).

The spin−spin coupling of the ^{199}Hg nucleus with the proton and carbon nuclei of the organomercurials provides the most important characteristics of their ^{1}H and ^{13}C{^{1}H} NMR spectra, which can serve as convenient tools for detecting the redox-transmetalation products formed during the mercury drop test or corresponding control experiments. In the ^{1}H NMR spectra of arylmercuric chlorides, the most useful characteristic may be the $^3J_{HHg}$ constants based on the efficient ^{199}Hg nucleus interaction with the *ortho*-proton of the metalated aromatic ring, possessing rather large values: For example, $^3J_{HHg}$ constants equal to 187−223 Hz were found for mercurials **2b**, **3b**, **5b**, and **6b** (Table 3). The characteristic satellites due to the interaction of mercury with the *meta*- and *para*-protons of the same aromatic ring have much lower spin−spin coupling constants: 42−78 Hz for $^4J_{HHg}$ and 17 Hz for $^5J_{HHg}$. Moreover, mercury satellite detection is often problematic due to strong overlapping signals in the ^{1}H NMR spectra of compounds with complicated hydrocarbon skeletons.

Therefore, in a practical sense, the ^{13}C{^{1}H} NMR spectra are more useful for organomercurial detection in solutions. The signals of the mercury-bonded carbon of the metalated aromatic ring in the ^{13}C{^{1}H} NMR spectra of arylmercuric chlorides **2b**, **3b**, **5b**, and **6b** are flanked by satellites arising from ^{13}C−^{199}Hg spin−spin coupling, with very high $^1J_{CHg}$ constant values of 2378−2567 Hz. The remaining ^{199}Hg−^{13}C coupling constants for the metalated aromatic ring in the spectra of **1b**−**3b**, **5b**, and **6b** decrease from 214 to 19 Hz in accordance with the standard regularity[61a] in the sequence $^1J_{CHg} \gg {}^3J_{CHg} > {}^2J_{CHg} > {}^4J_{CHg}$ (Table 3).

The spectral characteristics of the side chain are primarily of interest to clarify the fate of the mercuracycle after organomercuric chloride dissolution. The ^{1}H NMR spectra of mercurials **1b**−**6b** are not suitable to solve this problem, since only in the case of arylimine-derived mercurial **1b** was the ^{199}Hg coupling with the α-methine proton detected with a long-range $^4J_{HHg}$ constant equal to 10 Hz. The main reason for a rather effective ^{199}Hg−^{1}H interaction in this case lies in the sp^2-hybridization of the α-carbon atom providing the ideal planarity of the Hg−C^4═C^5−C$^\alpha$−H chain. However, an additional contribution from the spin−spin coupling via Hg ← N═C$^\alpha$−H bonds ($^3J_{HHg}$ constant) inside the mercuracycle cannot be excluded since, in the crystal of **1b**, the shortest Hg−N bond distance was 2.586 Å, compared to 2.620−2.824 Å for mercurials **2b**−**5b** (Table 2). The ^{13}C{^{1}H} NMR spectra of all mercurials **1b**−**5b** reveal the interaction of the α-carbon atom with mercury(II) with $^3J_{CHg}$ constant values ranging from 118 to 26 Hz. We propose that such variations can be mainly explained by the known dihedral angle dependence of the J_{CHg} constant values,[46d] although in the case of mercurial **1b**, an additional contribution from Hg−N−$^\alpha$C spin−spin coupling ($^2J_{CHg}$ constant) cannot be excluded.

In principle, the most reliable information regarding the retention of nitrogen-to-mercury coordination in solution could be obtained from the ^{199}Hg-^{13}C coupling constants for exocyclic *N*-substituents. However, only in the ^{13}C{^{1}H} NMR spectra of mercurial **5b** bearing an oxazolinyl *N*-donor were satellites detected for a very distant asymmetric carbon atom (C^9), with a formal $^5J_{CHg}$ constant equal to 14 Hz. This can be explained by a more efficient spin−spin coupling through the chain Hg−C^1═C^2−C$^\alpha$═N−C^9 of double bonds ($^5J_{CHg}$ constant), with a possible contribution from Hg−N−C^9 spin−spin coupling ($^2J_{CHg}$ constant). Thus, only mercurials with (sp^2) nitrogen donors showed weak indications of possible chelation of such ligands. The absence of any signs of the ^{199}Hg−^{13}C interaction with the NMe$_2$ carbons of **2b**−**4b**, with the *ipso*-carbon of the *N*-aryl substituent in **1b** or with C^{11} carbon of the pyridine ring in **6b** points to a predominantly dechelated state of mercurials **2b**−**4b** and **6b** in solution at ambient temperature.

Dynamic NMR of the Organomercuric Chlorides. Dynamic NMR of the organomercuric chlorides was undertaken to clarify the possibility of retaining Hg···N interactions in solution and to estimate the quantitative aspects of this process. For this goal, mercurated tertiary amines (R_C)-**2b** and (R_C,S_{pl})*-**4b** bearing two diastereotopic NMe groups were used as examples. Previously, the dynamic behavior was studied at a qualitative level only for arylmercuric chlorides (S_C)-**3b**[39] and (R_C)-**C**[50] and for their α-unsubstituted ferrocenyl analogue of type **D** where R = Me (*rac*-**D^1**, Chart 3).[53,53b]

The temperature dependence of the ^{1}H NMR spectra of the mercurial (R_C)-**2b** in $CDCl_3$ solution was studied in the range from −45 to 55 °C. It is important that even at ambient temperature, the spectrum indicated the nonequivalence of the diastereotopic *N*-methyl groups: two broadened signals were observed for their protons at δ_H 2.15 and 2.46 ppm, with their half width equal to 120 Hz (Figures S36 and S38). The slow exchange limit was achieved at −15 °C, when two narrow anisochronous signals ($\Delta\nu_{1/2}$ 3.6 Hz) were observed for *N*-methyl protons at 2.05 and 2.65 ppm. The simulated ^{1}H NMR spectra of (R_C)-**2b** and the exchange rate constants are presented in Figure S36. The following activation parameters of the dynamic process for mercurial (R_C)-**2b** were found: $\Delta G_{298}^{\ddagger}$ = 13.7 ± 0.2 kcal/mol, $\Delta H_{298}^{\ddagger}$ = 16.0 ± 0.1 kcal/mol, and $\Delta S_{298}^{\ddagger}$ = 7.6 ± 0.2 cal/mol/deg (the Eyring plot is presented on the Figure S37).

For comparison, it should be noted that only one resonance was observed for the NMe$_2$ group in the ^{1}H NMR spectra of analogues (S_C)-**3b**[39] and (R_C)-**C**[50] measured at room temperature, while two anisochronous resonances for this group were observed only at temperatures below −70 or −60 °C, respectively. Such dynamic behavior is explained by the retention of Hg−N coordination, resulting in a blocked inversion at the nitrogen on the NMR time scale at low

DOI: 10.1021/acs.organomet.8b00363
Organometallics XXXX, XXX, XXX−XXX

temperatures, while this bond cleavage at ambient temperature offers an opportunity for fast pyramidal inversion at the nitrogen.

However, significant differences in the dynamic behavior of mercurial (R_C)-**2b** and its analogues (S_C)-**3b** and (R_C)-**C** allow us to assume a considerable influence of steric effects on the lability extent of the related organomercuric chlorides. The equilibrium between species bearing a monodentate aryl ligand or a bidentate weakly κ^2*C,N*-bonded amine may be significantly shifted toward the latter for the (R_C)-**2b** complex derived from naphth-1-ylethylamine to avoid the steric hindrance between C(8) hydrogen of the naphthalene ring and the α-Me or Me_2N groups of the free-rotating *N*-decoordinated arylalkylamine ligand $(L^2)^-$.

In contrast to α-naphthylethylamine derivative (R_C)-**2b**, the ^{1}H NMR spectrum of its ferrocenyl analogue (R_C,S_{pl})*-**4b** in CD_2Cl_2 contains only one rather narrow singlet of NMe_2 group protons (Figure S39). Its broadening was observed at temperatures below −30 °C, and only at −85 °C did this signal shape become close to that expected for the moment of coalescence. Although we were unable to measure the exact difference between the chemical shifts of the diastereotopic NMe_2 group signals at the slow exchange limit, the upper limit of the magnitude of the dynamic process barrier was estimated as $\Delta G_{233}^{\ddagger} < 9 \pm 1$ kcal/mol.

For comparison, it should be noted that in the case of α-unsubstituted analogue *rac*-**D**[1] (Chart 3), dimethylamino group protons remain isochronous even at −80 °C; the authors propose that such fluxional behavior means that the intramolecular Hg···N interaction is not preserved in solution.[53b] The difference in the degree of dynamic mobility of mercurials (R_C)-**2b** and (R_C,S_{pl})*-**4b** may be partly attributed to the geometric requirements of their arylene frameworks, which are six- or five-membered, respectively. In reality, the sum of the angles Hg−C^1−C^2 and C^1−C^2−C^α increases from 236.8° for (R_C)-**2b** in crystalline form (240° is expected for an ideal hexagon) to 240.5° for (R_C,S_{pl})*-**4b** and to an average value of 253° for a series of α-unsubstituted analogues *rac*-**D** (Chart 3, Tables S3 and S4), which is close to the value of 252° expected for an ideal pentagon.

The most important consequence of these geometry changes is the increasing Hg···C^α distance from 3.149 Å in (R_C)-**2b** to 3.320 Å in (R_C,S_{pl})*-**4b** and 3.571 Å in α-unsubstituted analogues *rac*-**D**. This should lead to the removal of the nitrogen atom from mercury and reduce the ability of the *N*-donor to interact with the metal.

CONCLUSION

The main goal of the presented research was to dispel the myth of narrow mercury(0) selectivity and emphasize the absolute necessity of control experiments that exclude the possibility of cyclopalladated (pre)catalyst killing by metallic mercury as the reason for a positive mercury poisoning test. The almost complete disregard for this mandatory requirement[1a,b,d,38b] is based on the widespread misconception that completely rejects the possibility of mercury(0) interaction with homogeneous molecular complexes containing d^8 metals in high oxidation states.[1c,7,9] Contrary to these assumptions, our investigation of the interaction of mercury(0) with diverse *C,N*-palladacycles has shown the formation of organomercuric chlorides as a result of their redox-transmetalation. We have established a significant dependence of this process's effectiveness on the palladacycle structure, reaction conditions, mercury/palladium ratio and base presence. These circumstances require strict compliance with the conditions required for the control experiments and mercury drop test conditions.

The structure of the isolated organomercurials was convincingly confirmed by ^{1}H, ^{13}C{^{1}H}, and ^{199}Hg{^{1}H} NMR spectroscopy and crystallography. The behavior of the *C,N*-mercuracycles bearing a rather weak and labile N···Hg bond was discussed on the basis of the temperature dependence of the NMR spectra and the thermodynamic parameters of the dechelation process, calculated by the DFT method. The set of the presented spectral data for the isolated organomercurials, especially the ^{199}Hg-^{13}C spin−spin coupling constant values, can serve as a convenient tool for detecting the related redox-transmetalation products formed during the mercury drop test or corresponding control experiments. After ensuring that all the necessary conditions are met, the ubiquitous mercury poisoning test ceases to be the simplest possible test, but these conditions are an important way to avoid erroneous mechanistic conclusions from its application.

Since the rich (but unfortunately forgotten) mercury(0) chemistry[62] is not limited to the considered reactions (*vide supra*), and the library of cyclopalladated (pre)catalysts is not limited to the azapalladacycles, it is also necessary to determine all the possible transformations of other *C,E*-palladacycles and other participants in the catalytic system (including substrates, reagents, and bases) occurring during the mercury poisoning test. This research is now in progress by our group.

EXPERIMENTAL SECTION

General Information. The ^{1}H (400.0 MHz), ^{13}C{^{1}H} (100.6 MHz), and ^{119}Hg{^{1}H} (71.5 MHz) NMR spectra were recorded on the Agilent 400-MR spectrometer. The measurements were carried out at ambient temperature (unless otherwise specified) in $CDCl_3$ solutions. The chemical shifts are reported in δ-scale in parts per million relative to residual $CHCl_3$ (δ 7.26 ppm for ^{1}H or δ 77.16 ppm for ^{13}C{^{1}H} NMR) and relative to $(CH_3)_2Hg$ as an external reference for the ^{119}Hg{^{1}H} NMR; constant *J* values are presented in Hz. The signal assignment was based on the gCOSY, gHMQC, and gHMBC experiments. Dynamic NMR study was performed using line-shape analysis of the spectra acquired at different temperatures. The exchange rate constant for each temperature was determined using simulation algorithm DNMR3 program SPINWORKS 4.1.[63] The activation parameters for the exchange process were calculated using Eyring equation. Optical rotations were measured with a A. Krüss Optronic P8000 polarimeter in a 0.25 dm cell at 20 °C. The melting points were measured on an Electrothermal IA 9000 series device. The TLC on Silufol UV-254 was used to follow the course of reactions. Compound purification was performed using short dry column[64] or flash-chromatography on silica gel (60, Fluka).

Toluene was dried over $CaCl_2$, refluxed over Na and then distilled under argon. Hexane and light petroleum ether (40−70 °C) were distilled from Na under argon. Anhydrous MeOH was prepared by distillation from MeONa. Diethyl ether was dried over KOH, then refluxed and distilled from Na/benzophenone under argon. Chloroform and dichloromethane were passed through a short Al_2O_3 column (L 40/250, Fluka 60) and distilled from P_2O_5 under argon. $CDCl_3$ (from Aldrich) was distilled from CaH_2 under argon just before using. KF (from Acrus) and metallic mercury of >99.999% purity (from Abcr) were used as received.

Dimeric cyclopalladated complexes (R_{pl})- and *rac*-di-μ-chloro-bis{4-(*N*-2,6-dimethylphenyl)iminomethyl[2.2]paracyclophane-5-yl-*C,N*}-dipalladium(II), (R_{pl})-**1a** and *rac*-**1a**;[65] (R_C)-di-μ-chloro-bis{1-(1′-(*N,N*-dimethylamino)ethyl)naphthyl-2*C,N*}dipalladium(II), (R_C)-**2a**;[66] (S_C)-di-μ-chloro-bis{2-(1′-(*N,N*-dimethylamino)ethyl)phenyl-*C,N*}dipalladium(II), (S_C)-**3a**;[67] di-μ-chloro-bis[2-{1′-(dimethylamino)ethyl}ferrocenyl-*C,N*]-dipalladium(II), *rac*-**4a**;[40] (S_C)-di-μ-chlorobis-{2-[(4′-*tert*-butyl)oxazolin-2′-yl]phenyl-*C,N*}-

DOI: 10.1021/acs.organomet.8b00363
Organometallics XXXX, XXX, XXX−XXX

dipalladium(II), (S_C)-**5a**;[68] and di-μ-chloro-bis{2-(pyridinyl-2′-oxy)-phenyl-*C*,*N*}dipalladium(II), **6a**,[69] were prepared by known methods.

***Caution**: Despite the arylmercury(II) compounds being generally quite stable, the toxicity of organomercury(II) compounds is well-documented and appropriate precautions should be taken in the handling of all organomercury(II) compounds.*

Redox-Transmetalation Reactions of *C,N*-Palladacycles with Mercury(0). *(R_{pl})-{4-(N-2,6-Dimethylphenyl)iminomethyl[2.2]-paracyclophane-5-yl-C,N}mercury(II) chloride, (R_{pl})-**1b**.* A mixture of enantiopure dimer (R_{pl})-**1a** (0.0151 g, 0.0157 mmol) and metallic mercury excess (1.8917 g, 9.4307 mmol, 277 equiv) in toluene (15 mL) was intensively stirred at 90 °C for 1 h in air. At this stage the palladacycle was completely reacted (TLC data). After removing the metallic mercury, the light-yellow solution was evaporated in a vacuum to dryness. The crude product was purified using short dry column chromatography on silica (h = 4 cm, d = 2 cm; eluents: petroleum ether, petroleum ether/diethyl ether 10:1, 7:1 and 5:1) to afford arylmercuric chloride (R_{pl})-**1b** (0.0162 g, 0.0282 mmol, 90% yield) as light-yellow amorphous powder. Data for (R_{pl})-**1b**: mp 236−239 °C. R_f = 0.28 (petroleum ether/dichloromethane 3:2); 0.27 (toluene). $[\alpha]_D^{22}$ +507.6° (c 0.11, dichloromethane). Anal. Calcd for $C_{25}H_{24}NClHg$ requires: C 52.27; H 4.21. Found: C 52.67; H 4.32. ^{1}H NMR ($CDCl_3$): Aromatic protons of the [2.2]paracyclophane moiety: δ 6.43 (dd, 1H, $^3J_{HH}$ 7.8, $^4J_{HH}$ 1.9, H^{13}), 6.56 (dd, 1H, $^3J_{HH}$ 7.8, $^4J_{HH}$ 1.9, H^{12}), 6.57 (d, 1H, $^3J_{HH}$ 7.7, H^7), 6.59 (dd, 1H, $^3J_{HH}$ 7.8, $^4J_{HH}$ 1.9, H^{16}), 6.63 (dd, 1H, $^3J_{HH}$ 7.8, $^4J_{HH}$ 1.9, H^{15}), 6.83 (dd, 1H, $^3J_{HH}$ 7.7, $^4J_{HHg}$ 78.0, H^8); methylene protons of the [2.2]paracyclophane moiety: 2.89 (ddd, 1H, $^2J_{HH}$ 13.3, $^3J_{HH}$ 6.6, $^3J_{HH}$ 10.3, H^{10s}), 3.06 (ddd, 1H, $^2J_{HH}$ 14.0, $^3J_{HH}$ 6.6, $^3J_{HH}$ 10.4, H^{9a}), 3.17 (ddd, 1H, $^2J_{HH}$ 13.5, $^3J_{HH}$ 4.0, $^3J_{HH}$ 10.9, H^{2s}), 3.24 (ddd, 1H, $^2J_{HH}$ 13.5, $^3J_{HH}$ 4.0, $^3J_{HH}$ 10.8, H^{1a}), 3.27 (ddd, 1H, $^2J_{HH}$ 13.5, $^3J_{HH}$ 3.7, $^3J_{HH}$ 10.9, H^{1s}), 3.29 (ddd, 1H, $^2J_{HH}$ 13.3, $^3J_{HH}$ 2.1, $^3J_{HH}$ 10.4, H^{10a}), 3.39 (ddd, 1H, $^2J_{HH}$ 13.5, $^3J_{HH}$ 3.7, $^3J_{HH}$ 10.8, H^{2a}), 3.59 (ddd, 1H, $^2J_{HH}$ 14.0, $^3J_{HH}$ 2.1, $^3J_{HH}$ 10.3, H^{9s}); side chain protons: 2.30 (s, 6H, 2Me), 7.01−7.05 (m, 1H, A part of AB_2 system, J_{AB} 7.5, *para*-H of C_6H_3), 7.13 (ps. d, 2H, B part of AB_2 system, J_{AB} 7.5, *meta*-H, C_6H_3), 8.63 (s, 1H, J_{HHg} 10.4, C*H*═N). ^{13}C{^{1}H} NMR ($CDCl_3$): Aromatic carbons of the [2.2]paracyclophane moiety: δ 131.69 (C^{12}), 133.01 (C^{15}), 133.16 (C^{16}), 133.66 (C^{13}), 135.93 (J_{CHg} 202, C^8), 136.11 (J_{CHg} 30, C^7), 138.85 (C^{11}), 138.11 (J_{CHg} 48, C^5), 139.10 (C^{14}), 144.04 (J_{CHg} 164, C^6), 153.80 (C^4), 146.36 (J_{CHg} 91, C^3); methylene carbons of the [2.2]paracyclophane moiety: 33.54 (J_{CHg} 23, C^9), 35.79 (C^1), 36.17 (C^{10}), 41.31 (J_{CHg} 125, C^2); side chain carbons: 19.04 (Me), 124.73 (*p*-C), 128.30 (*o*-C), 128.44 (*m*-C), 149.42 (*i*-C), 161.96 (J_{CHg} 118, CH═N). ^{199}Hg{^{1}H} NMR ($CDCl_3$): δ_{Hg} −977.6 ppm (s).

*rac-{4-(N-2,6-Dimethylphenyl)iminomethyl[2.2]-paracyclophane-5-yl-C,N}mercury(II) Chloride, rac-**1b**.* A suspension of dimer *rac*-**1a** (0.0300 g, 0.0312 mmol) and metallic mercury excess (4.134 g, 20.61 mmol, 330 equiv) was intensively stirred for 3 h in boiling toluene (15 mL) in air, which was accompanied by color changing from yellow to light-yellow. After removing the metallic mercury, the light-yellow solution was evaporated in a vacuum to dryness. The crude product was purified using short dry column chromatography on silica (h = 4 cm, d = 2.5 cm; petroleum ether, petroleum ether/dichloromethane 2:1, 1:1) to afford individual transmetalation product *rac*-**1b** (0.0322 g, 0.0560 mmol, 90%) as a yellow amorphous powder. Crystalline complex *rac*-**1b** suitable for X-ray diffraction studies was obtained by slow evaporation of its solution in a solvent mixture toluene/petroleum ether/chloroform. Data for *rac*-**1b**: mp (decomp.) 239−241 °C. R_f = 0.27 (toluene); 0.28 (petroleum ether/dichloromethane 3:2).

*(R_C)-{1-(1′-(N,N-Dimethylamino)ethyl)naphthyl-2C,N}mercury(II) Chloride, (R_C)-**2b**.* A mixture of dimer (R_C)-**2a** (0.0400 g, 0.0588 mmol) and metallic mercury excess (7.780 g, 38.79 mmol, 330 equiv) in toluene (15 mL) was intensively stirred at 70 °C for 9 h under argon, accompanied by color changing from bright yellow to almost colorless. After removing the metallic mercury, the solution was evaporated in a vacuum to dryness. The crude product was purified using short dry column chromatography on silica (h = 4 cm, d = 2.5 cm; eluents light petroleum ether and light petroleum ether/diethyl ether 3:1 mixture) to afford transmetalation product (R_C)-**2b** (0.0411 g, 0.0946 mmol, 81%) as almost colorless crystalline powder. The almost colorless needle-like crystals of complex (R_C)-**2b** suitable for X-ray diffraction studies were obtained by slow crystallization from a solvent mixture dichloromethane/diethyl ether/petroleum ether. Data for (R_C)-**2b**: mp 159−161 °C. R_f = 0.59 (light petroleum ether/diethyl ether 4:1). $[\alpha]_D^{22}$ − 40° (c 0.25, CH_2Cl_2). Anal. Calcd for $C_{14}H_{16}NClHg$ requires: C 38.72; H 3.71; N 3.22. Found: C 38.68; H 3.60; N 3.16. ^{1}H NMR ($CDCl_3$): Protons of the aromatic moiety: δ_H 7.48 (ddd, 1H, $^3J_{HH}$ 8.1, $^3J_{HH}$ 6.9, $^3J_{HH}$ 6.9, $^4J_{HH}$ 1.4, H^6), 7.53 (ddd, 1H, $^3J_{HH}$ 8.3, $^4J_{HH}$ 1.8, H^7), 7.56 (dd, 1H, $^3J_{HH}$ 8.1, $^3J_{HHg}$ 187, H^3), 7.72 (dd, 1H, $^3J_{HH}$ 8.1, $^3J_{HHg}$ 54, H^4), 7.87 (dd, 1H, $^3J_{HH}$ 8.1, $^4J_{HH}$ 1.8, H^5), 8.05 (br.d, 1H, $^3J_{HH}$ 8.3, H^8); side chain protons: 1.42 (d, 3H, $^3J_{HH}$ 6.7, α-Me), 2.16 (br. s, $\Delta\nu_{1/2} \geq$ 120 Hz, 3H, NMe), 2.56 (br. s, $\Delta\nu_{1/2} \geq$ 120 Hz, 3H, NMe), 4.48 (q, 1H, $^3J_{HH}$ 6.7, α-CH). ^{13}C{^{1}H} NMR ($CDCl_3$): Carbons of the aromatic moiety: δ_C 129.04 (J_{CHg} 9, C^5), 121.83 (J_{CHg} 20, C^8), 125.89 (J_{CHg} 6, C^6), 126.32 (J_{CHg} 18, C^7), 126.93 (J_{CHg} 208, C^4), 131.56 (J_{CHg} 194, C^9), 133.69 (J_{CHg} 134, C^3), 133.78 (C^{10}), 145.01 (J_{CHg} 2495, C^2), 147.09 (J_{CHg} 51, C^1); side chain carbons: 23.45 (α-Me), 42.3 (br. s, NMe_2), 44.2 (br. s, NMe_2), 60.97 (J_{CHg} 106, α-CH). ^{199}Hg{^{1}H} NMR ($CDCl_3$): δ_{Hg} −905.3 ppm (s).

*(S_C)-{2-(1′-(N,N-Dimethylamino)ethyl)phenyl-C,N}mercury(II) Chloride, (S_C)-**3b**.* A mixture of dimer (S_C)-**3a** (0.0400 g, 0.0689 mmol) and metallic mercury excess (9.127 g, 45.50 mmol, 330 equiv) in toluene (15 mL) was intensively stirred at 70 °C for 8 h in air. After removing the metallic mercury, the solution was evaporated in a vacuum to dryness. The crude product was purified using short dry column chromatography on silica (h = 4 cm, d = 2.5 cm; eluents light petroleum ether and light petroleum ether/diethyl ether 2:1 mixture) to afford transmetalation product (S_C)-**3b** (0.0412 g, 0.1072 mmol, 78%) as almost colorless amorphous powder. Data for (S_C)-**3b**: mp 75−78 °C. R_f = 0.36 (light petroleum ether/diethyl ether 4:1). $[\alpha]_D^{22}$ + 51° (c 0.25, CH_2Cl_2). Anal. Calcd for $C_{10}H_{14}NClHg$ requires: C 31.26; H 3.67; N 3.64. Found: C 31.41; H 3.80; N 3.48. ^{1}H NMR ($CDCl_3$): protons of the aromatic moiety: δ_H 7.22 (m, 2H, H^3, H^5), 7.23 (m, 1H, H^4), 7.41 (m, 1H, $^3J_{HHg}$ 223, H^6); side chain protons: 1.31 (d, 3H, $^3J_{HH}$ 6.7, α-Me), 2.27 (s, 6H, NMe_2), 3.51 (q, 1H, $^3J_{HH}$ 6.7, $^3J_{HHg}$ 24, α-CH). ^{13}C{^{1}H} NMR ($CDCl_3$): carbons of the aromatic moiety: δ_C 128.50 (J_{CHg} 169, C^3), 128.81 (J_{CHg} 31, C^4), 132.21 (J_{CHg} 214, C^5), 127.32 (J_{CHg} 140, C^6), 147.04 (J_{CHg} 2464, C^1), 150.73 (J_{CHg} 49, C^2); side chain carbons: 21.77 (α-Me), 42.52 (NMe_2), 66.05 (J_{CHg} 93, α-CH). ^{199}Hg{^{1}H} NMR ($CDCl_3$): δ_{Hg} −933.4 ppm (s).

*rac-[2-{1′-(Dimethylamino)ethyl}ferrocenyl-C,N]mercury(II) Chloride, rac-**4b**.* A mixture of dimer *rac*-**4a** (0.180 g, 0.2261 mmol) and metallic mercury excess (27.00 g, 134.6 mmol, 298 equiv) in toluene (20 mL) was intensively stirred at room temperature for 3.5 h under argon. After 50 min after start of the reaction the precipitate of the cyclopalladated dimer is completely dissolved. After removal of metallic mercury and its washing with toluene (3 × 5 mL), the solutions were evaporated in a vacuum to dryness. The chromatographic purification of the crude product using short dry column chromatography on silica (h = 3 cm, d = 1.5 cm; eluents toluene/ethyl acetate 5:1, ethyl acetate, methanol) affords individual cyclomercurated complex *rac*-**4b** (0.180 g, 0.3657 mmol, 81%) as red-brown oil. After multistage crystallization from methanol major diastereomeric racemate (R_CS_{pl})*-**7b** was isolated as orange crystals (118 mg, 0.2397 mmol, 53%) with mp 115 °C. Anal. Calcd for $C_{14}H_{18}ClFeHgN$ requires: C 34.16; H 3.69. Found: C 34.19; H 3.81.

Spectral Data for Isolated (R_CS_{pl}) Diastereomer.* ^{1}H NMR ($CDCl_3$): δ_H 1.12 (d, 3H, $^3J_{HH}$ 6.8, α-Me), 2.12 (s, 6H, NMe_2), 3.92 (q, 1H, $^3J_{HH}$ 6.8, α-CH), 4.06 (dd, 1H, J_{HHg} 51, $^3J_{HH}$ 2.3, $^4J_{HH}$ 1.1, H^5), 4.08 (s, 5H, Cp), 4.22 (dd, 1H, J_{HHg} 42, $^3J_{HH}$ 2.5, $^3J_{HH}$ 2.3, H^4), 4.35 (br. dd, 1H, J_{HHg} 31, $^3J_{HH}$ 2.5, $^4J_{HH}$ 1.1, H^3). ^{13}C{^{1}H} NMR ($CDCl_3$): δ_C 9.08 (α-Me), 39.19 (N*Me*$_2$), 59.81 (J_{CHg} 34, α-CH), 67.86 ($^2J_{CHg}$ 156, C^5), 69.07 ($^3J_{CHg}$ 206, C^4), 69.38 (Cp), 72.27 ($^3J_{CHg}$ 253, C^3), 87.14 (C^1), 95.14 ($^2J_{CHg}$ 131, C^2). ^{199}Hg{^{1}H} NMR ($CDCl_3$): δ_{Hg} −733.9 ppm (s).

Spectral Data for Diastereomer Mixture. ^{1}H NMR ($CDCl_3$): δ_H of major diastereomer: 1.12 (d, $^3J_{HH}$ 6.8, 3H, α-Me), 2.12 (s, 6H, NMe_2), 3.93 (q, $^3J_{HH}$ 6.6, 1H, α-H), 4.06 (dd, $^3J_{HH}$ 2.3, $^4J_{HH}$ 1.1, 1H, H^5), 4.08 (s, Cp), 4.23 (dd, $^3J_{HH}$ 2.4, $^3J_{HH}$ 2.4, 1H, H^4), 4.36 (ddd, $^3J_{HH}$ 2.4, $^4J_{HH}$

DOI: 10.1021/acs.organomet.8b00363
Organometallics XXXX, XXX, XXX−XXX

1.1, $^4J_{HH}$ 0.4, 1H, H^3); δ_H of minor diastereomer: 1.31 (d, $^3J_{HH}$ 6.8, 3H, α-Me), 2.37 (s, 6H, NMe$_2$), 3.26 (q, $^3J_{HH}$ 6.7, 1H, α-H), 4.12 (m, 2H, H3, H5), 4.17 (s, Cp), 4.33 (dd, $^3J_{HH}$ 2.4, $^3J_{HH}$ 2.4, 1H, H^4). ^{13}C{^{1}H} NMR (CDCl$_3$): δ_C of major diastereomer: 9.19 (α-Me), 39.14 (N*Me*$_2$), 59.93 ($^3J_{CHg}$ 33, α-CH), 67.88 ($^2J_{CHg}$ 156, C^5), 69.21 ($^3J_{CHg}$ 206, C^4), 69.41 (Cp), 72.53 ($^3J_{CHg}$ 248, C^3), 87.08 (C^1), 94.57 (C^2); δ_C of minor diastereomer: 12.34 (α-Me), 41.21 (N*Me*$_2$), 56.00 ($^3J_{CHg}$ 26, α-CH), 66.17 ($^2J_{CHg}$ 160, C^5), 68.94 (Cp), 70.13 ($^3J_{CHg}$ 208, C^4), 71.62 ($^3J_{CHg}$ 260, C^3), 81.92 (C^1), 98.40 (C^2). ^{199}Hg{^{1}H} NMR (CDCl$_3$): δ_{Hg} −732.8 (major diastereomer), −684.8 (minor diastereomer).

*(S$_C$)-{2-[2′-(4-tert-Butyl)oxazolinyl]phenyl-C,N}mercury(II) Chloride, (S$_C$)-**5b***. A mixture of dimer (S$_C$)-**5a** (0.0400 g, 0.0581 mmol) and metallic mercury excess (7.70 g, 38.4 mmol, 330 equiv) in toluene (15 mL) was intensively stirred at room temperature for 4 days under argon. After removing the metallic mercury, the solution was evaporated in a vacuum to dryness. The crude product was purified using short dry column chromatography on silica (h = 4 cm, d = 2.5 cm; eluents light petroleum ether and light petroleum ether/diethyl ether 2:1 mixture) to afford transmetalation product (S$_C$)-**5b** (0.0362 g, 0.08259 mmol, 71%) as almost colorless crystalline powder. Data for (S$_C$)-**5b**: mp 150−151 °C. $[\alpha]_D^{22}$ + 22° (c 0.25, CH$_2$Cl$_2$). R_f = 0.64 (light petroleum ether/diethyl ether 4:1). Anal. Calcd for C$_{13}$H$_{16}$NClOHg requires: C 35.62; H 3.68; N 3.20. Found: C 35.36; H 3.71; N 3.15. ^{1}H NMR (CDCl$_3$): Protons of the aromatic moiety: δ_H 7.51 (ddd, 1H, J_{HHg} 49, $^3J_{HH}$ 7.4, $^3J_{HH}$ 7.4, $^4J_{HH}$ 1.4, H^5), 7.41 (ddd, 1H, J_{HHg} 206, $^3J_{HH}$ 7.4, $^4J_{HH}$ 1.4, $^5J_{HH}$ 0.6, H^6), 7.35 (ddd, 1H, J_{HHg} 17, $^3J_{HH}$ 7.4, $^3J_{HH}$ 7.8, $^4J_{HH}$ 1.4, H^4), 7.88 (ddd, 1H, J_{HHg} 62, $^3J_{HH}$ 7.8, $^4J_{HH}$ 1.4, $^5J_{HH}$ 0.6, H^3); side chain protons: 0.96 (s, 9H, ^{t}Bu), 4.01 (dd, 1H, $^3J_{HH}$ 8.8, $^3J_{HH}$ 10.2, J_{HHg} 3, α-C^{9}H), 4.28 (dd, 1H, $^2J_{HH}$ 8.7, $^3J_{HH}$ 8.8, C^{8}H$_2$), 4.46 (dd, 1H, $^2J_{HH}$ 8.7, $^3J_{HH}$ 10.2, C^{8}H$_2$). ^{13}C{^{1}H} NMR (CDCl$_3$): Carbons of the aromatic moiety: δ_C 128.54 ($^3J_{CHg}$ 145, C^3), 128.54 ($^4J_{CHg}$ 29, C^4), 132.14 (J_{CHg} 40, C^7), 132.21 ($^3J_{CHg}$ 209, C^5), 136.96 ($^2J_{CHg}$ 132, C^6), 150.62 ($^1J_{CHg}$ 2567, C^1), 167.76 ($^2J_{CHg}$ 105, C^2); side chain carbons: 26.05 (*Me*$_3$C), 33.77 (CMe$_3$), 70.43 (C^{8}H$_2$), 75.54 (J_{CHg} 14, α-C^{9}H). ^{199}Hg{^{1}H} NMR (CDCl$_3$): δ_{Hg} −1056.6 ppm (s).

*{2-(Pyridinyl-2′-oxy)phenyl-C,N}mercury(II) Chloride, **6b***. A mixture of dimer **6a** (0.0400 g, 0.0641 mmol) and metallic mercury excess (8.49 g, 42.3 mmol, 330 equiv) in toluene (15 mL) was intensively stirred at 70 °C for 1 h in air. After removing the metallic mercury, the solution was evaporated in a vacuum to dryness. The crude product was purified using short dry column chromatography on silica (h = 4 cm, d = 2.5 cm; eluents: light petroleum ether and light petroleum ether/diethyl ether 1:1 and 1:3 mixtures) to afford individual transmetalation product **6b** (0.0481 g, 0.1184 mmol, 92%) as almost colorless amorphous powder. After slow recrystallization from DCM/Et$_2$O/petroleum ether, complex **6b** was isolated (0.0363 g, 0.0894 mmol, 70%) as almost colorless thin needle-like crystals. Data for **6b**: mp 158−161 °C. R_f = 0.24 (light petroleum ether/diethyl ether 1:1). Anal. Calcd for C$_{11}$H$_8$NOClHg requires: C 32.52; H 1.98. Found: C 32.30; H 2.09. ^{1}H NMR (CDCl$_3$): δ_H 6.94 (br.d, 1H, $^3J_{HH}$ 8.2, H^8), 7.04 (ddd, 1H, $^3J_{HH}$ 5.0, $^3J_{HH}$ 7.2, $^4J_{HH}$ 0.9, H^{10}), 7.15 (d, 1H, $^3J_{HH}$ 8.0, H^3), 7.23 (m, 1H, H^5), 7.35 (m, 1H, $^3J_{HHg}$ 208, H^6), 7.36 (m, 1H, H^4), 7.71 (ddd, 1H, $^3J_{HH}$ 8.2, $^3J_{HH}$ 7.2, $^4J_{HH}$ 2.0, H^9), 8.19 (ddd, 1H, $^3J_{HH}$ 5.0, $^4J_{HH}$ 2.0, $^5J_{HH}$ 0.6, H^{11}). ^{13}C{^{1}H} NMR (CDCl$_3$): δ_C 112.57 (C^8), 119.47 (C^{10}), 121.50 ($^3J_{CHg}$ 104, C^3), 125.38 ($^3J_{CHg}$ 193, C^5), 130.48 ($^4J_{CHg}$ 19, C^4), 136.65 ($^2J_{CHg}$ 78, C^6), 140.06 (C^9), 142.59 ($^1J_{CHg}$ 2378, C^1), 147.56 (C^{11}), 157.06 ($^2J_{CHg}$ 30, C^2), 163.07, C^7). ^{199}Hg{^{1}H} NMR (CDCl$_3$): δ_{Hg} −1115.0 ppm (s).

Computational Details. The geometries of molecules, transition states, and intermediates were fully optimized by means of density functional theory (DFT) calculations. The PBE functional[70] and scalar-relativistic theory were used, the latter employing the four-component spin-free Hamiltonian derived by Dyall[71] and applied variationally. The full electron double size basis set was used. The numbers of contracted and primitive functions used respectively {2,1}/{6,2} for H, {3,2,1}/{10,7,3} for C, N, and O, {4,3,1}/{15,11,3} for Cl, {8,7,5,2}/{30,29,20,14} for Hg.[72] Stationary points on the potential energy surface (PES) were identified by analyzing Hessians. The thermodynamic functions (Gibbs energies, G) at 298.15 K were calculated using an approximation of restricted rotator and harmonic oscillator. Reaction paths were found by the intrinsic reaction coordinate (IRC) method.[73] All calculations were performed using the MBC100k cluster at the Joint Supercomputer Center (JSCC) (Moscow, Russia) with the use of the PRIRODA04 program written by Laikov.[74]

X-ray Diffraction Study of Mercurials. X-ray diffraction data were collected at the "Belok" beamline of the Kurchatov Synchrotron Radiation Source (National Research Center "Kurchatov Institute", Moscow, Russian Federation) using a Rayonix SX165 CCD detector at λ = 0.96990 Å (for (R_C)-**2b**), 0.96260 Å (for (R_CS_{pl})*-**4b**), and 0.80246 Å (for (S_C)-**5b** and **6b**). All data sets were collected at 100 K. In total, 480−720 frames were collected with an oscillation range of 1.0° in the φ scanning mode using two different orientations for each crystal. The semiempirical correction for absorption was applied using the Scala program.[75] The data were indexed and integrated using the utility iMOSFLM from the CCP4 software suite.[76] For details, see Table S14. The structures were solved by intrinsic phasing modification of direct methods[77] and refined by a full-matrix least-squares technique on F^2 with anisotropic displacement parameters for all non-hydrogen atoms. All hydrogen atoms were placed in calculated positions and refined within the riding model with fixed isotropic displacement parameters [U_{iso}(H) = 1.5U_{eq}(C) for the methyl groups and 1.2U_{eq}(C) for the other groups]. All calculations were carried out using the SHELXTL program.[78]

■ ASSOCIATED CONTENT

Supporting Information

The Supporting Information is available free of charge on the ACS Publications website at DOI: 10.1021/acs.organomet.8b00363.

Cartesian coordinates of calculated complexes reported in this study (XYZ)

Additional experimental details; bond lengths and angles, figures and tables giving ^{1}H, ^{13}C, and ^{199}Hg NMR spectra, gCOSY, gHMQC and gHMBC NMR; VT NMR spectra and DFT data; tables of X-ray diffraction and NMR data for known analogues (PDF)

Accession Codes

CCDC 1843928−1843931 contain the supplementary crystallographic data for this paper. These data can be obtained free of charge via www.ccdc.cam.ac.uk/data_request/cif, or by emailing data_request@ccdc.cam.ac.uk, or by contacting The Cambridge Crystallographic Data Centre, 12 Union Road, Cambridge CB2 1EZ, UK; fax: +44 1223 336033.

■ AUTHOR INFORMATION

Corresponding Author

*E-mail: dunina@org.chem.msu.ru. Fax: +7 (495) 932 8846. Tel.: +7(495) 939 5376.

ORCID

Olga N. Gorunova: 0000-0001-6947-4763

Ivan M. Novitskiy: 0000-0002-2675-3348

Victor N. Khrustalev: 0000-0001-8806-2975

Valery V. Dunina: 0000-0003-4289-0294

Notes

The authors declare no competing financial interest.

■ ACKNOWLEDGMENTS

We thank the Russian Foundation of Basic Researches (grant no. 18-03-01026a). The NMR part of this work was supported by M. V. Lomonosov Moscow State University "Program of Development" (Y.K.G., V.A.R.).

DOI: 10.1021/acs.organomet.8b00363
Organometallics XXXX, XXX, XXX−XXX

REFERENCES

(1) (a) Crabtree, R. H. Resolving Heterogeneity Problems and Impurity Artifacts in Operationally Homogeneous Transition Metal Catalysts. *Chem. Rev.* **2012**, *112*, 1536−1554. (b) Schmidt, A. F.; Kurokhtina, A. A. Distinguishing between the Homogeneous and Heterogeneous Mechanisms of Catalysis in the Mizoroki−Heck and Suzuki−Miyaura Reactions: Problems and Prospects. *Kinet. Catal.* **2012**, *53*, 714−730. (c) Phan, N. T. S.; van der Sluys, M.; Jones, C. W. On the Nature of the Active Species in Palladium Catalyzed Mizoroki−Heck and Suzuki−Miyaura Couplings − Homogeneous or Heterogeneous Catalysis, A Critical Review. *Adv. Synth. Catal.* **2006**, *348*, 609−679. (d) Widegren, J. A.; Finke, R. G. A Review of the Problem of Distinguishing True Homogeneous Catalysis from Soluble or other Metal-Particle Heterogeneous Catalysis under Reducing Conditions. *J. Mol. Catal. A: Chem.* **2003**, *198*, 317−341.

(2) (a) Drost, R. M.; Rosar, V.; Marta, S. D.; Lutz, M.; Demitri, N.; Milani, B.; de Bruin, B.; Elsevier, C. J. Pd-Catalyzed Z-Selective Semihydrogenation of Alkynes: Determining the Type of Active Species. *ChemCatChem* **2015**, *7*, 2095−2107. (b) Bolliger, J. L.; Blacque, O.; Frech, C. M. Rationally Designed Pincer-Type Heck Catalysts Bearing Aminophosphine Substituents: Pd^{IV} Intermediates and Palladium Nanoparticles. *Chem. - Eur. J.* **2008**, *14*, 7969−7977.

(3) Paal, C.; Hartmann, W. Über den Einfluß von Fremdstoffen auf die Aktivität der Katalysatoren. IV. Versuche mit Palladiumhydrosol in Qegenwart von Queksilber und Quecksilberoxyd. *Ber. Deutsch. Ber. Dtsch. Chem. Ges.* **1918**, *51*, 711−737.

(4) (a) Steckel, J. A. Density Functional Theory Study of Mercury Adsorption on Metal Surfaces. *Phys. Rev. B: Condens. Matter Mater. Phys.* **2008**, *77*, 115412. (b) Campbell, K. C.; Hislop, J. S. Mercury Adsorption, Catalyst Poisoning, and Reactivation Phenomena on Metal Catalysts. *J. Catal.* **1969**, *13*, 12−19.

(5) (a) Anton, D. R.; Crabtree, R. H. Dibenzo[*a*,*e*]cyclooctatetraene in a Proposed Test for Heterogeneity in Catalysts Formed from Soluble Platinum Group Metal Complexes. *Organometallics* **1983**, *2*, 855−859. (b) Foley, P.; DiCosimo, R.; Whitesides, G. M. Mechanism of Thermal Decomposition of Dineopentylbis(triethylphosphine)platinum(II): Formation of Bis(triethy1phosphine)-3,3-dimethy1p1atinacyc1obutane. *J. Am. Chem. Soc.* **1980**, *102*, 6713−6725.

(6) Schwartz, J. Alkane Activation by Oxide-Bound Organorhodium Complexes. *Acc. Chem. Res.* **1985**, *18*, 302−308.

(7) (a) Yu, K.; Sommer, W.; Weck, M.; Jones, C. W. Silica and Polymer-tethered Pd−SCS-pincer Complexes: Evidence for Precatalyst Decomposition to Form Soluble Catalytic Species in Mizoroki−Heck Chemistry. *J. Catal.* **2004**, *226*, 101−110. (b) Sommer, W. J.; Yu, K.; Sears, J. S.; Ji, Y.; Zheng, X.; Davis, R. J.; Sherrill, C. D.; Jones, C. W.; Weck, M. Investigations into the Stability of Tethered Palladium(II) Pincer Complexes during Heck Catalysis. *Organometallics* **2005**, *24*, 4351−4361.

(8) (a) Stein, J.; Lewis, L. N.; Gao, Y.; Scott, R. A. In situ Determination of the Active Catalyst in Hydrosilylation Reactions Using Highly Reactive Pt(0) Catalyst Precursors. *J. Am. Chem. Soc.* **1999**, *121*, 3693−3703. (b) van Asselt, R.; Elsevier, C. J. Homogeneous Catalytic Hydrogenation of Alkenes by Zero-valent Palladium Complexes of *cis*-Fixed Dinitrogen Ligands. *J. Mol. Catal.* **1991**, *65*, L13−L19. (c) Jones, R. A.; Real, F. M.; Wilkinson, G.; Galas, A. M. R.; Hursthouse, M. B. Further Chemistry of Trimethylphosphine Complexes of Rhodium(I): X-Ray Crystal Structures of Dodeca-(trimethy1phosphine)tetrarhodiumhexamercury, $Hg_6Rh_4(PMe_3)_{12}$, and *trans*-Chlorobis(trimethy1phosphine)(triphenylphosphine)-rhodium(I). *J. Chem. Soc., Dalton Trans.* **1981**, 126−131.

(9) (a) Shiels, R. A.; Jones, C. W. A Convergence of Homogeneous and Heterogeneous Catalysis: Immobilized Organometallic Catalysts. *Model Systems in Catalysis* **2010**, *20*, 441−455. (b) Yu, K.; Sommer, W.; Richardson, J. M.; Weck, M.; Jones, C. W. Evidence that SCS Pincer Pd(II) Complexes are only Precatalysts in Heck Catalysis and the Implications for Catalyst Recovery and Reuse. *Adv. Synth. Catal.* **2005**, *347*, 161−171.

(10) (a) Beletskaya, I. P.; Cheprakov, A. V.; Colacot, T. J. Modern Heck Reactions. *New Catalysis Series* **2014**, *21*, 355−478. (b) Bedford, R. B. Palladacyclic Pre-Catalysts for Suzuki Coupling, Buchwald−Hartwig Amination and Related Reactions. In *Palladacycles. Synthesis, Characterization and Applications*; Dupont, J., Pfeffer, M., Eds.; Wiley-VCH: Weinheim, 2008; pp 209−225. (c) Dupont, J.; Consorti, C. S.; Spencer, J. The Potential of Palladacycles: More Than Just Precatalysts. *Chem. Rev.* **2005**, *105*, 2527−2571. (d) Beletskaya, I. P.; Cheprakov, A. V. Palladacycles in Catalysis − a Critical Survey. *J. Organomet. Chem.* **2004**, *689*, 4055−4082. (e) Beletskaya, I. P.; Cheprakov, A. V. The Heck Reaction as a Sharpening Stone of Palladium Catalysis. *Chem. Rev.* **2000**, *100*, 3009−3066.

(11) (a) Ramírez-Rave, S.; Morales-Morales, D.; Grévy, J.-M. Microwave Assisted Suzuki-Miyaura and Mizoroki-Heck Cross-couplings Catalyzed by non-Symmetric Pd(II) CNS Pincers Supported by Iminophosphorane Ligands. *Inorg. Chim. Acta* **2017**, *462*, 249−255. (b) Das, U.; Pattanayak, P.; Patra, D.; Brandão, P.; Felix, V.; Chattopadhyay, S. Design, Synthesis and Properties of Orthopalladated Complexes: Proheterogeneous Catalyst. *Polyhedron* **2016**, *110*, 165−171. (c) Zhang, H.; Lei, A. Palladium(IV) Chemistry Supported by Pincer Type Ligands. *Dalton Trans* **2011**, *40*, 8745−8754. (d) Avila-Sorrosa, A.; Estudiante-Negrete, F.; Hernández-Ortega, S.; Toscano, R. A.; Morales-Morales, D. Buchwald−Hartwig C−N Cross Coupling Reactions Catalyzed by a Pseudo-Pincer Pd(II) Compound. *Inorg. Chim. Acta* **2010**, *363*, 1262−1268. (e) Gerber, R.; Blacque, O.; Frech, C. M. Suzuki Cross-Coupling Reactions Catalyzed by an Aliphatic Phosphine-Based Pincer Complex of Palladium: Evidence for a Molecular Mechanism. *ChemCatChem* **2009**, *1*, 393−400. (f) Hossain, Md.A.; Lucarini, S.; Powell, D.; Bowman-James, K. Ditopic Double Pincer Palladacycle Catalyst for C-C Coupling. *Inorg. Chem.* **2004**, *43*, 7275−7277. (g) Sjövall, S.; Wendt, O. F.; Andersson, C. Synthesis, Characterisation and Catalytic Investigation of a New Type of PC(sp^3)P Pincer Pd(II) Complex. *J. Chem. Soc., Dalton Trans.* **2002**, 1396−1400. (h) Morales-Morales, D.; Redón, R.; Yung, C.; Jensen, C. M. High Yield Olefination of a Wide Scope of Aryl Chlorides Catalyzed by The Phosphinito Palladium PCP Pincer Complex: [PdCl-{$C_6H_3(OPPr^i_2)_2$-2,6}]. *Chem. Commun.* **2000**, 1619−1620. (i) Ohff, M.; Ohff, A.; van der Boom, M. E.; Milstein, D. Highly Active Pd(II) PCP-Type Catalysts for the Heck Reaction. *J. Am. Chem. Soc.* **1997**, *119*, 11687−1688.

(12) (a) Lucio-Martínez, F.; Adrio, L. A.; Polo-Ces, P.; Ortigueira, J. M.; Fernández, J. J.; Adams, H.; Pereira, M. T.; Vila, J. M. Palladacycle Catalysis: an Innovation to the Suzuki−Miyaura Cross-Coupling Reaction. *Dalton Trans.* **2016**, *45*, 17598−17601. (b) Gerber, R.; Blacque, O.; Frech, C. M. Negishi Cross-Coupling Reaction Catalyzed by an Aliphatic, Phosphine Based Pincer Complex of Palladium. Biaryl Formation via Cationic Pincer-Type Pd^{iv} Intermediates. *Dalton Trans.* **2011**, *40*, 8996−9003. (c) Blacque, O.; Frech, C. M. Pincer-Type Heck Catalysts and Mechanisms Based on Pd^{IV} Intermediates: A Computational Study. *Chem. - Eur. J.* **2010**, *16*, 1521−1531. (d) Sundermann, A.; Uzan, O.; Martin, J. M. L. Computational Study of a New Heck Reaction Mechanism Catalyzed by Palladium(II/IV) Species. *Chem. - Eur. J.* **2001**, *7*, 1703−1711.

(13) (a) Camasso, N. M.; Canty, A. J.; Ariafard, A.; Sanford, M. S. Experimental and Computational Studies of High-Valent Nickel and Palladium Complexes. *Organometallics* **2017**, *36*, 4382−4393. (b) Xu, L.-M.; Li, B.-J.; Yang, Z.; Shi, Z.-J. Organopalladium(IV) chemistry. *Chem. Soc. Rev.* **2010**, *39*, 712−733. (c) Albrecht, M.; van Koten, G. Platinum Group Organometallics Based on "Pincer" Complexes: Sensors, Switches, and Catalysts. *Angew. Chem., Int. Ed.* **2001**, *40*, 3750−3781.

(14) (a) Vicente-Hernández, I.; Chicote, M.-T.; Vicente, J.; Bautista, D. A New Type of Oxidative Addition of an Iodoarene to a Pd(II) Complex. *Chem. Commun.* **2016**, *52*, 594−596. (b) Martínez-Martínez, A.-J.; Chicote, M.-T.; Bautista, D.; Vicente, J. Synthesis of Palladium-(II), -(III), and -(IV) Complexes with Acyclic Diaminocarbene Ligands. *Organometallics* **2012**, *31*, 3711−3719. (c) Juliá-Hernández, F.; Arcas, A.; Vicente, J. Providing Support in Favor of the Existence of a Pd^{II}/Pd^{IV} Catalytic Cycle in a Heck-Type Reaction. *Chem. - Eur. J.* **2012**, *18*, 7780−7786. (d) Vicente, J.; Arcas, A.; Juliá-Hernández, F.; Bautista, D. Synthesis of a Palladium(IV) Complex by Oxidative

DOI: 10.1021/acs.organomet.8b00363
Organometallics XXXX, XXX, XXX−XXX

Addition of an Aryl Halide to Palladium(II) and Its Use as Precatalyst in a C−C Coupling Reaction. *Angew. Chem., Int. Ed.* **2011**, *50*, 6896−6899.

(15) Joshi, H.; Prakash, O.; Sharma, A. K.; Sharma, K. N.; Singh, A. K. Suzuki Coupling Reactions Catalyzed with Palladacycles and Palladium(II) Complexes of 2-Thiophenemethylamine-Based Schiff Bases: Examples of Divergent Pathways for the Same Ligand. *Eur. J. Inorg. Chem.* **2015**, 1542−1552.

(16) (a) Błaszczyk, I.; Gniewek, A.; Trzeciak, A. M. Orthometallated Palladium Trimers in C−C Coupling Reactions. *J. Organomet. Chem.* **2012**, *710*, 44−52. (b) Błaszczyk, I.; Gniewek, A.; Trzeciak, A. M. Monomeric Triphenylphosphite Palladacycles with N-Imidazole Ligands as Catalysts of Suzuki-Miyaura and Sonogashira Reactions. *J. Organomet. Chem.* **2011**, *696*, 3601−3607. (c) Peris, E.; Loch, J. A.; Mata, J.; Crabtree, R. H. A Pd Complex of a Tridentate Pincer CNC Bis-Carbene Ligand as a Robust Homogenous Heck Catalyst. *Chem. Commun.* **2001**, 201−202.

(17) (a) Singh, M. P.; Saleem, F.; Pal, R. S.; Singh, A. K. Palladacycles Having Normal and Spiro Chelate Rings Designed from Bi- and Tridentate Ligands with an Indole Core: Structure, Synthesis and Applications as Catalysts. *New J. Chem.* **2017**, *41*, 11342−11352. (b) Avila-Sorrosa, A.; Jiménez-Vázquez, H. A.; Reyes-Arellano, A.; Pioquinto-Mendoza, J. R.; Toscano, R. A.; González-Sebastián, L.; Morales-Morales, D. Novel Synthesis of a Non-Symmetric N^1CN^2-Pd(II) Pincer Complex by a Tandem Reaction Using a *Meta*-Hydroxylated Imine Ligand. *J. Organomet. Chem.* **2016**, *819*, 69−75.

(18) Sharma, A. K.; Joshi, H.; Bhaskar, R.; Kumar, S.; Singh, A. K. Palladacycles of Sulfated and Selenated Schiff Bases of Ferrocene-Carboxaldehyde as Catalysts for O-Arylation and Suzuki−Miyaura Coupling. *Dalton Trans.* **2017**, *46*, 2485−2496.

(19) (a) Olsson, D.; Wendt, O. F. Suzuki Reaction Catalysed by a $Pc_{sp3}P$ Pincer Pd(II) Complex: Evidence for a Mechanism Involving Molecular Species. *J. Organomet. Chem.* **2009**, *694*, 3112−3115. (b) Bolliger, J. L.; Blacque, O.; Frech, C. M. Short, Facile, and High-Yielding Synthesis of Extremely Efficient Pincer-Type Suzuki Catalysts Bearing Aminophosphine Substituents. *Angew. Chem., Int. Ed.* **2007**, *46*, 6514−6517.

(20) (a) Olsson, D.; Nilsson, P.; El Masnaouy, M.; Wendt, O. F. A Catalytic and Mechanistic Investigation of a PCP Pincer Palladium Complex in the Stille Reaction. *J. Chem. Soc., Dalton Trans.* **2005**, 1924−1929. (b) Nilsson, P.; Wendt, O. F. Kinetic Investigation of a $PC(sp^3)P$ Pincer Palladium (II) Complex in the Heck Reaction. *J. Organomet. Chem.* **2005**, *690*, 4197−4202. (c) Rosol, M.; Moyano, A. 1′-Carbopalladated-4-ferrocenyl-1,3-oxazolines as Catalysts for Heck Reactions: Further Evidence in Support of the Pd(0)/Pd(II) Mechanism. *J. Organomet. Chem.* **2005**, *690*, 2291−2296.

(21) (a) Baier, H.; Kelling, A.; Schilde, U.; Holdt, H.-J. Investigation of the Catalytic Activity of a 2-Phenylidenepyridine Palladium(II) Complex Bearing 4,5-Dicyano-1,3-bis(mesityl)imidazol-2-ylidene in the Mizoroki-Heck Reaction. *Z. Anorg. Allg. Chem.* **2016**, *642*, 140−147. (b) Baier, H.; Kelling, A.; Holdt, H.-J. PEPPSI-Effect on Suzuki−Miyaura Reactions Using 4,5-Dicyano-1,3-dimesitylimidazol-2-ylidene-Palladium Complexes: A Comparison between *trans*-Ligands. *Eur. J. Inorg. Chem.* **2015**, 1950−1957. (c) Baier, H.; Metzner, Ph.; Körzdörfer, Th.; Kelling, A.; Holdt, H.-J. Efficient Palladium(II) Precatalysts Bearing 4,5-Dicyanoimidazol-2-ylidene for the Mizoroki−Heck Reaction. *Eur. J. Inorg. Chem.* **2014**, 2952−2960. (d) Poulain, A.; Neels, A.; Albrecht, M. Palladium Complexes Containing Potentially Chelating Pyridylidene-Type Carbene Ligands. *Eur. J. Inorg. Chem.* **2009**, 1871−1881. (e) Consorti, C. S.; Flores, F. R.; Dupont, J. Kinetics and Mechanistic Aspects of the Heck Reaction Promoted by a CN-Palladacycle. *J. Am. Chem. Soc.* **2005**, *127*, 12054−12065. (f) Consorti, C. S.; Zanini, M. L.; Leal, S.; Ebeling, G.; Dupont, J. Chloropalladated Propargyl Amine: A Highly Efficient Phosphine-Free Catalyst Precursor for the Heck Reaction. *Org. Lett.* **2003**, *5*, 983−986.

(22) Sabounchei, S. J.; Ahmadi, M.; Panahimehr, M.; Bagherjeri, F. A.; Nasri, Z. Phosphine Mono- and bis-Ylide Palladacycles as Homogeneous Molecular Precatalysts: Simple and Efficient Protocol Greatly Facilitate Suzuki and Heck Coupling Reactions. *J. Mol. Catal. A: Chem.* **2014**, *383-384*, 249−259.

(23) Zim, D.; Nobre, S. M.; Monteiro, A. L. Suzuki Cross-Coupling Reaction Catalyzed by Sulfur-Containing Palladacycles: Formation of Palladium Active Species. *J. Mol. Catal. A: Chem.* **2008**, *287*, 16−23.

(24) (a) Lipke, M. C.; Woloszynek, R. A.; Ma, L.; Protasiewicz, J. D. *m*-Terphenyl Anchored Palladium Diphosphinite PCP-Pincer Complexes That Promote the Suzuki-Miyaura Reaction Under Mild Conditions. *Organometallics* **2009**, *28*, 188−196. (b) Eberhard, M. R. Insights into the Heck Reaction with PCP Pincer Palladium(II) Complexes. *Org. Lett.* **2004**, *6*, 2125−2128.

(25) Bergbreiter, D. E.; Osburn, P. L.; Frels, J. D. Mechanistic Studies of SCS-Pd Complexes Used in Heck Catalysis. *Adv. Synth. Catal.* **2005**, *347*, 172−184.

(26) Sigeev, A. S.; Peregudov, A. S.; Cheprakov, A. V.; Beletskaya, I. P. The Palladium Slow-Release Pre-Catalysts and Nanoparticles in the "Phosphine-Free" Mizoroki−Heck and Suzuki−Miyaura Reactions. *Adv. Synth. Catal.* **2015**, *357*, 417−429.

(27) (a) Bhaskar, R.; Sharma, A. K.; Yadav, M. K.; Singh, A. K. Sonogashira (Cu and Amine Free) and Suzuki Coupling in Air Catalyzed via Nanoparticles Formed in situ from Pd(II) Complexes of Chalcogenated Schiff Bases of 1-Naphthaldehyde and their Reduced Forms. *Dalton Trans.* **2017**, *46*, 15235−15248. (b) Rao, G. K.; Kumar, A.; Singh, M. P.; Singh, A. K. Palladium(II) Complex of an Organotellurium Ligand as a Catalyst for Suzuki Miyaura Coupling: Generation and Role of Nano-Sized Pd_3Te_2. *J. Organomet. Chem.* **2014**, *749*, 1−6. (c) Rao, G. K.; Kumar, A.; Kumar, S.; Dupare, U. B.; Singh, A. K. Palladacycles of Thioethers Catalyzing Suzuki−Miyaura C−C Coupling: Generation and Catalytic Activity of Nanoparticles. *Organometallics* **2013**, *32*, 2452−2458.

(28) Ananikov, V. P.; Beletskaya, I. P. Toward the Ideal Catalyst: From Atomic Centers to a "Cocktail" of Catalysts. *Organometallics* **2012**, *31*, 1595−1604.

(29) (a) Gorunova, O. N.; Grishin, Yu. K.; Ilyin, M. M., Jr.; Kochetkov, K. A.; Churakov, A. V.; Kuźmina, L. G.; Dunina, V. V. Enantioselective Catalysis of Suzuki reaction with Planar-Chiral *CN*-Palladacycles: Competition of two Catalytic Cycles. *Russ. Chem. Bull.* **2017**, *66*, 282−292. (b) Gorunova, O. N.; Livantsov, M. V.; Grishin, Y. K.; Ilyin, M. M., Jr.; Kochetkov, K. A.; Churakov, A. V.; Kuz'mina, L. G.; Khrustalev, V. N.; Dunina, V. V. Evidence on Palladacycle-Retaining Pathway for Suzuki Coupling. Inapplicability of Hg-drop Test for Palladacycle Catalysed Reactions. *J. Organomet. Chem.* **2013**, *737*, 59−63.

(30) (a) Wu, Y.; Huo, Sh.; Gong, J.; Cui, X.; Ding, L.; Ding, K.; Du, Ch.; Liu, Y.; Song, M. Studies on the Cyclometallation of Ferrocenylimines. *J. Organomet. Chem.* **2001**, *637-639*, 27−46. (b) Cui, X. L.; Wu, Y. J.; Du, Ch. X.; Yang, L. R.; Zhu, Y. Transmetallation Reactions of Planar Chiral Cyclopalladated Ferrocenylimines with Metallic Mercury. *Tetrahedron: Asymmetry* **1999**, *10*, 1255−1262.

(31) Vedejs, E.; Salomon, M. F. Preparation, Stereochemistry, and Rearrangement of Mercurials in the Norbornenyl-Nortricyclyl System. *J. Org. Chem.* **1972**, *37*, 2075−2079.

(32) Wu, Y. J.; Cui, X. L.; Hou, J. J.; Yang, L. R.; Wang, M.; Du, C. X.; Zhu, Y. Transmetallation Reactions of Planar Chiral Cyclopalladated and Cyclomercurated Ferrocenylimines with Metallic Tin. *Acta Chim. Sin.* **2000**, *58*, 871−875.

(33) (a) Nesmeyanov, A. N.; Blinova, V. A.; Shchirina-Eingorn, I. V.; Kritskaya, I. I. Synthesis of Some Difficulty Accessible Allylic Organomercury Compounds. *Bull. Acad. Sci. USSR, Div. Chem. Sci.* **1977**, *26*, 2178−2180. (b) Rubezhov, A. Z.; Voronchikhina, L. I.; Gubin, S. P. Synthesis of *m*- and *p*-Fluorophenylallyl Mercury Chlorides. *Bull. Acad. Sci. USSR, Div. Chem. Sci.* **1972**, *21*, 2060−2062. (c) Nesmeyanov, A. N.; Rubezhov, A. Z.; Leites, V.; Gubin, S. P. The Reactions of Metallic Mercury with π-Allyl Compounds of Ni, Pd and Pt. *J. Organomet. Chem.* **1968**, *12*, 187−198. (d) Gubin, S. P.; Rubezhov, A. Z.; Denisovich, L. I.; Nesmeyanov, A. N. Reaction of Metallic Mercury with π-Allyl Compounds of Palladium. *Bull. Acad. Sci. USSR, Div. Chem. Sci.* **1966**, *15*, 1630.

DOI: 10.1021/acs.organomet.8b00363
Organometallics XXXX, XXX, XXX−XXX

(34) (a) Costa, R. D.; Cossich, E. S.; Tavares, C. R. G. Influence of the Temperature, Volume and Type of Solution in the Mercury Vaporization of Dental Amalgam Residue. *Sci. Total Environ.* **2008**, *407*, 1−6. (b) Palaniappan, R. Indirect Spectrophotometric Determination of Palladium(II). *Pak. J. Sci. Ind. Res.* **1989**, *32* (2), 79−81.
(35) Whitesides, G. M.; Hackett, M.; Brainard, R. L.; Lavalleye, J.-P. P. M.; Sowinski, A. F.; Izumi, A. N.; Moore, S. S.; Brown, D. W.; Staudt, E. M. Suppression of Unwanted Heterogeneous Platinum(0)-Catalyzed Reactions by Poisoning with Mercury(0) in Systems Involving Competing Homogeneous Reactions of Soluble Organoplatinum Compounds: Thermal Decomposition of Bis(triethylphosphine)-3,3,4,4-tetramet hylplatinacyclopentane. *Organometallics* **1985**, *4*, 1819−1830.
(36) Lewis, L. N.; Lewis, N. Platinum-Catalyzed Hydrosilylation - Colloid Formation as the Essential Step. *J. Am. Chem. Soc.* **1986**, *108*, 7228−7231.
(37) (a) Butin, K. P.; Gunkin, I. F.; Petri, R.; Beletskaya, I. P.; Reutov, O. A. Exchange of Organometallic Compounds with Mercury Metal. VII. Interaction of Di-*p*-Anisylthallium Chloride with Mercury in Pyridine, Ethylenediamine and Dimethylsulfoxide; Prevaling Role of Homogeneous Reaction. *J. Organomet. Chem.* **1976**, *114*, 239−250. (b) Reutov, O. A.; Butin, K. P. "Organic Calomels" and Other Organometallic Compounds as Intermediates in Transmetallation Reactions of Organometallic Compounds with Mercury Metal. *J. Organomet. Chem.* **1975**, *99*, 171−184. (c) Butin, K. P.; Strelets, V. V.; Gunkin, I. F.; Beletskaya, I. P.; Reutov, O. A. Exchange of Organometallic Compounds with Mercury Metal. VI. Substituted Diarylthallium Cations; Evidence for Intermediate Ar−Tl^{+}−Hg−Ar Species. *J. Organomet. Chem.* **1975**, *85*, 123−130. (d) Butin, K. P.; Strelets, V. V.; Beletskaya, I. P.; Reutov, O. A. Exchange of Organometallic Compounds with Mercury Metal. V. The Interaction of Diethyltallium Chloride with Mercury. *J. Organomet. Chem.* **1974**, *64*, 189−191. (e) Gilman, H.; Jones, R. G. Relative Reactivities of Organometallic Compounds. XXVII. Triphenylthallium. *J. Am. Chem. Soc.* **1939**, *61*, 1513−1515.
(38) (a) Crabtree, R. H. Deactivation in Homogeneous Transition Metal Catalysis: Causes, Avoidance, and Cure. *Chem. Rev.* **2015**, *115*, 127−150. (b) Dyson, P. J. Arene Hydrogenation by Homogeneous Catalysts: Fact or Fiction? *Dalton Trans.* **2003**, 2964−2974.
(39) (a) Attar, S.; Nelson, J. H.; Fischer, J. Crystal Structures of Chiral Halo{2[l-(*S*)-(dimethylamino)ethyl]phenyl-C^{1},*N*}mercury(II) Complexes. *Organometallics* **1995**, *14*, 4776−4780. (b) van der Ploeg, A. F. M. J.; van der Kolk, C. E. M.; van Koten, G. Arylmercury(II) Compounds Involving Intramolecular Coordination *via* 2-Me_2NCH_2- and Chiral (*S*)-2-Me_2NCHMe-ring Substituents. *J. Organomet. Chem.* **1981**, *212*, 283−290.
(40) Sokolov, V. I.; Troitskaya, L. L.; Reutov, O. A. Asymmetric Induction in the Course of Internal Palladation of Enantiomeric 1-Dimethylaminomethylferrocene. *J. Organomet. Chem.* **1977**, *133*, C28−C30.
(41) Bondi, A. van der Waals Volumes and Radii. *J. Phys. Chem.* **1964**, *68*, 441−451.
(42) Canty, A. J.; Deacon, G. B. The van der Waals Radius of Mercury. *Inorg. Chim. Acta* **1980**, *45*, L225−L227.
(43) Pyykkö, P.; Straka, M. *Ab initio* Studies of the Dimers $(HgH_2)_2$ and $(HgMe_2)_2$. Metallophilic Attraction and the van der Waals Radii of Mercury. *Phys. Chem. Chem. Phys.* **2000**, *2*, 2489−2493.
(44) (a) Batsanov, S. S. Van der Waals Radii of Elements. *Inorg. Mater.* **2001**, *37*, 871−885. (b) Batsanov, S. S. On the Additivity of van der Waals Radii. *J. Chem. Soc., Dalton Trans.* **1998**, 1541−1546.
(45) Kuz'mina, L. G.; Bokii, N. G.; Struchkov, Y. T. The Structural Chemistry of Organic Compounds of Mercury and Its Analogues (Zinc and Cadmium). *Russ. Chem. Rev.* **1975**, *44*, 73−85.
(46) (a) Gabbaï, F. P.; Burress, C. N.; Melaimi, M.-A.; Taylor, T. J. Mercury and Cadmium Organometallics. In *Comprehensive Organometallic Chemistry III*; Mingos, D. M. P., Crabtree, R. H., Eds.; Elsevier: Oxford, 2007; Vol. 2, pp 419−462. (b) Casas, J. S.; García-Tasende, M. S.; Sordo, J. Structural Aspects of the Coordination Chemistry of Organothallium(III) and Organomercury(II) derivatives. *Coord. Chem. Rev.* **1999**, *193-195*, 283−359. (c) Holloway, C. E.; Melník, M. Mercury Organometallic Compounds. Classification and Analysis of Crystallographic and Structural Data. *J. Organomet. Chem.* **1995**, *495*, 1−31. (d) Wardell, J. L. Mercury. In *Comprehensive Organometallic Chemistry*; Wilkinson, G.; Stone, F. G. A.; Abel, E. W., Eds.; Pergamon: Oxford, 1982; Vol. 2, pp 863−978. (e) Grdenić, D. The Structural Chemistry of Mercury. *Quart. Rev., Chem. Soc.* **1965**, *19*, 303−328.
(47) Baligar, R. S.; Sharma, S.; Singh, H. B.; Butcher, R. J. Synthesis and Structure of New Schiff Base Derivatives Obtained from 2-(Formylphenyl)mercury Bromide. *J. Organomet. Chem.* **2011**, *696*, 3015−3022.
(48) Das, Sh.; Singh, H. B.; Butcher, R. J. Isolation of Organomercury(II) Azides Stabilized by Intramolecular Coordination. *J. Organomet. Chem.* **2015**, *799−800*, 184−194.
(49) (a) Wu, Y. J.; Huo, S. Q.; Zhu, Y.; Yang, L. Cyclometallation of Ferrocenylimines. Part II. Studies on the Cyclomercuration of [l-(Arylimino)ethyl]ferrocenes and Related Structure-Reactivity Relationships. *J. Organomet. Chem.* **1994**, *481*, 235−242. (b) Shou, Q. H.; Yang, J. W.; Ying, Z.; Li, Y. *ortho*-Mercuration of Ferrocenylimines. *J. Organomet. Chem.* **1994**, *470*, 17−22.
(50) Gül, N.; Nelson, J. H. Synthesis and Structures of Chiral Halo[N,N-dimethyl-α-(2-naphthyl)ethylamine-3,C,N]mercury(II) complexes. *J. Mol. Struct.* **1999**, *475*, 121−130.
(51) (a) Dunina, V. V. Chiral Cyclopalladated Compounds: New Structures, Methodologies and Applications. A Personal Account. *Curr. Org. Chem.* **2011**, *15*, 3415−3440. (b) Alcock, N. W.; Hulmes, D. I.; Brown, J. M. Contrasting Behaviour of Related Palladium Complex-derived Resolving Agents. 8-H Conformational Locking of the 1-Naphthyl Side-chain. *J. Chem. Soc., Chem. Commun.* **1995**, 395−397.
(52) Cordero, B.; Gómez, V.; Platero-Prats, A. E.; Revés, V.; Echeverría, J.; Cremades, E.; Barragán, F.; Alvarez, S. Covalent Radii Revisited. *Dalton Trans.* **2008**, 2832−2838.
(53) (a) Wang, H.-X.; Li, Y.-J.; Wu, H.-F.; Gao, R.-Q.; Geng, F.-Y.; Yang, X.-L.; Wan, L.; Jin, R.; Cui, X.-L.; Wu, Y.-J. Ortho-Mercurated [({*N*-Methyl-*N*-arylamino}methyl)ferrocenes] and their Transpalladation. Crystal Structures of $[(\eta^5\text{-}C_5H_5)Fe\{\eta^5\text{-}C_5H_3(HgCl)CH_2N(CH_3)C_6H_4OCH_3\text{-}4\}]_2$, $[(\eta^5\text{-}C_5H_5)Fe\{\eta^5\text{-}C_5H_3(HgCl)CH_2N(CH_3)C_6H_4Cl\text{-}3\}]$ and $[(\eta^5\text{-}C_5H_4HgCl)Fe\{\eta^5\text{-}C_5H_4CH_2N(CH_3)C_6H_4Cl\text{-}4\}]$. *Polyhedron* **2006**, *25*, 3305−3311. (b) Seidel, N.; Jacob, K.; Fischer, A. K.; Merzweiler, K.; Wagner, C.; Fontani, M.; Zanello, P. [2-(*N*,*N*-Dimethylaminomethyl)ferrocenyl] as a Ligand towards Mercury. *J. Organomet. Chem.* **2001**, *630*, 149−156. (c) Kuz'mina, L. G.; Struchkov, Yu. T.; Troitskaya, L. L.; Sokolov, V. I. X-ray Diffraction Structural Study of Nonbonding Interactions and Coordination in Heteroorganic Compounds. Part XXVI. X-ray Diffraction Structural Study of 1-Chloromercuri-2-dimethylaminomethylferrocene. *J. Struct. Chem.* **1985**, *26*, 428−432.
(54) Apte, S. D.; Zade, S. S.; Singh, H. B.; Butcher, R. Contrasting Behavior of Bis[2-(4,4-dimethyl-2-oxazolinyl)phenyl] Chalcogenides (Se/Te) toward Mercuric Chloride: Facile Cleavage of the Te-C Bond. *Organometallics* **2003**, *22*, 5473−5477.
(55) Li, H.; Wei, K.; Du, Ch.; Zhu, Y.; Xu, Ch.; Wu, Y. Synthesis, Characterization and Crystal Structures of a New 2-Ferrocenylnaphthoxazole and its Mercurated Derivatives. *J. Organomet. Chem.* **2007**, *692*, 1033−1038.
(56) (a) Hamid, G.; Somaieh, Y.; Yunes, A.; Michal, D.; Vaclav, E.; Majid, R.; Neslihan, O. Complexation of 1,3-Dimorpholinopropane with Hg(II) and Zn(II) Salts: Syntheses, Crystal Structures and Antibacterial Studies. *Chin. J. Inorg. Chem.* **2015**, *31*, 1076−1084. (b) Neuba, A.; Herres-Pawlis, S.; Seewald, O.; Börner, J.; Heuwing, A. J.; Flörke, U.; Henkel, G. A Systematic Study on the Coordination Properties of the Guanidine Ligand Bis(tetramethylguanidino)propane with the Metals Manganese, Cobalt, Nickel, Zinc, Cadmium, Mercury, and Silver. *Z. Anorg. Allg. Chem.* **2010**, *636*, 2641−2649. (c) Tang, X.-Y.; Yuan, R.-X.; Ren, Zh-G.; Li, H.-X.; Zhang, Y.; Lang, J.-P. Interactions of a Cationic Mercury(II) Thiolate Complex $[Hg(Tab)_2](PF_6)_2$ with *N*-Donor Ligands. *Inorg. Chem.* **2009**, *48*, 2639−2651. (d) Choi, S.-N.; Kim, S.-Yu.; Ryu, H.-W.; Lee, Y.-M. Dichloro-

DOI: 10.1021/acs.organomet.8b00363
Organometallics XXXX, XXX, XXX−XXX

[(6R,7S,8S,14S)-(−)-sparteine-κ^2N,N']mercury(II). *Acta Crystallogr., Sect. C: Cryst. Struct. Commun.* **2005**, *61*, m504−m506.
(57) Musavi, S. A.; Montazerozohori, M.; Masoudiasl, A.; Naghiha, R.; Joohari, S.; Assoud, A. Crystal Structure, DNA Interaction and Thermal Analysis Data of Two New Antimicrobial Active Binuclear Cadmium and Mercury Complexes. *J. Mol. Struct.* **2017**, *1145*, 65−75.
(58) (a) Bader, R. F. W. A. Quantum Theory of Molecular Structure and Its Applications. *Chem. Rev.* **1991**, *91*, 893−928. (b) Bader, R. F. W. *Atoms in Molecules: A Quantum Theory*; Oxford University Press: New York, 1990.
(59) (a) Constable, E. C.; Cargill Thompson, A. M. W.; Leese, T. A.; Reese, D. G. F.; Tocher, D. A. Cyclometallation Reactions of 2-Phenylpyridine; Crystal and Molecular Structure of (2-{2-Pyridyl}-phenyl)palladium(II) Tetramer and (2-{2-Pyridyl}phenyl)mercury-(II) Tetramer. *Inorg. Chim. Acta* **1991**, *182*, 93−100. (b) Constable, E. C.; Leese, T. A.; Tocher, D. A. Polynuclear Intermediates in the Synthesis of Cyclometallated Complexes; the Crystal and Molecular Structure of (2-PyridylphenyI)mercury(II) Chloride Tetramer. *J. Chem. Soc., Chem. Commun.* **1989**, 570−571.
(60) Beleaga, A.; Bojan, V. R.; Pöllnitz, A.; Raţ, C. I.; Silvestru, C. Organomercury(II) and Tellurium(II) Compounds with the "Pincer" Ligand 2,6-$[O(CH_2CH_2)_2NCH_2]_2C_6H_3$ − Stabilization of an Unusual Organotellurium(II) Cationic Species. *Dalton Trans.* **2011**, *40*, 8830−8838.
(61) (a) Rowland, K. E.; Thomas, R. D. Carbon-13 and Mercury-199 NMR Data for Methyl-Substituted Bisaryl Mercury Compounds. *Magn. Reson. Chem.* **1985**, *23*, 916−919. (b) Wells, P. R.; Hawker, D. W. Mercury-199 NMR Chemical Shifts in Substituted Diphenylmercury and Phenylmercuric Chloride. *Org. Magn. Reson.* **1981**, *17*, 26−27. (c) Chisholm, M. H.; Godleski, S. Applications of Carbon-13 NMR in Inorganic Chemistry. *Prog. Inorg. Chem.* **2007**, *20*, 299−436. (d) Petrosyan, V. S.; Reutov, O. A. NMR Spectra and Structure of Organomercury Compounds. *J. Organomet. Chem.* **1974**, *76*, 123−169.
(62) (a) Crabtree, R. H. The Organometallic Chemistry of Alkanes. *Chem. Rev.* **1985**, *85*, 245−269. (b) Larock, R. C. Organomercurials in Organic Synthesis. *Tetrahedron* **1982**, *38*, 1713−1754. (c) Larock, R. C. Organomercury Compounds in Organic Synthesis. *Angew. Chem., Int. Ed. Engl.* **1978**, *17*, 27−37. (d) Zeller, K. P.; Straub, H. Organo-quecksilber-Verbindungen; In *Houben−Weyl's Methoden der Organischen Chemie*, 4th ed.; Straub, H., Zeller, K. P., Leditschke, H., Eds.; Thieme Verlag: Stuttgart, 1974; Band 13/2b, pp 96−100.
(63) Marat, K. *SPINWORKS 4 Software*; University of Manitoba: Winnipeg MB, Canada. https://home.cc.umanitoba.ca/~wolowiec/spinworks/.
(64) Sharp, J. T.; Gosney, I.; Rowley, A. G. *Practical Organic Chemistry − A Student Handbook of Techniques*; Chapman and Hall: London, 1989; Chapter 4.2.2d.
(65) Dunina, V. V.; Turubanova, E. I.; Livantsov, M. V.; Lyssenko, K. A.; Vorontsova, N. V.; Antonov, D.; Grishin, Y. K. Yu.; Grishin, Y. K. First enantiopure imine *CN*-palladacycle of non-metallocenic planar chirality with the [2.2]paracyclophane backbone. *Tetrahedron: Asymmetry* **2009**, *20*, 1661−1671.
(66) Allen, D. G.; McLaughlin, G. M.; Robertson, G. B.; Steffen, W. L.; Salem, G.; Wild, S. B. Resolutions Involving Metal Complexation. Preparation and Resolution of (*R*,*S*)-Methylphenyl(8-quinoly1)-phosphine and Its Arsenic Analogue. Crystal and Molecular Structure of $(+)_{589}$-[(*R*)-Dimethyl(1-ethyl-α-naphthyl)aminato-C^2,*N*]-[(*S*)-methylphenyl(8-quinolyl)phosphine]palladium(II) Hexafluorophosphate. *Inorg. Chem.* **1982**, *21*, 1007−1014.
(67) Tani, K.; Brown, L. D.; Ahmed, J.; Ibers, J. A.; Yokota, M.; Nakamura, A.; Otsuka, S. Chiral Metal Complexes. 4. Resolution of Racemic Tertiary Phosphines with Chiral Palladium(II) Complexes. The Chemistry of Diastereomeric Phosphine Pd(II) Species in Solution, and the Absolute Configuration of [(*S*)-Isopropyl-*tert*-butylphenylphosphine]-[(*R*)-*N*,*N*-dimethyl-α-(2-naphthyl)-ethylamine-3*C*,*N*]chloropalladium(II) Determined by X-Ray Diffraction. *J. Am. Chem. Soc.* **1977**, *99*, 7876−7886.
(68) Peterson, D. L.; Keuseman, K. J.; Kataeva, N. A.; Kuz'mina, L. G.; Howard, J. A. K.; Dunina, V. V.; Smoliakova, I. P. Homochiral Cyclopalladated Complexes of (*S*)-4-*tert*-Butyl-2-phenyl-2-oxazoline. X-ray Study of (*S*,*S*)-di-μ-Chloro-bis-{2-[2-(4-*tert*-butyl)oxazolinyl]-phenyl-*C*,*N*}dipalladium(II). *J. Organomet. Chem.* **2002**, *654*, 66−73.
(69) de Geest, D. J.; O'Keefe, B. J.; Steel, P. J. Cyclometallated Compounds. XIII. Cyclopalladation of 2-Phenoxypyridine and Structurally-related Compounds. *J. Organomet. Chem.* **1999**, *579*, 97−105.
(70) Perdew, J. P.; Burke, K.; Ernzerhof, M. Generalized Gradient Approximation Made Simple. *Phys. Rev. Lett.* **1996**, *77*, 3865−3868.
(71) Dyall, K. G. An Exact Separation of the Spin-free and Spin-dependent Terms of the Dirac-Coulomb-Breit Hamiltonian. *J. Chem. Phys.* **1994**, *100*, 2118−2127.
(72) Laikov, D. N. A. New Class of Atomic Basis Functions for Accurate Electronic Structure Calculations of Molecules. *Chem. Phys. Lett.* **2005**, *416*, 116−120.
(73) Gonzalez, C.; Schlegel, H. B. Reaction Path Following in Mass-Weighted Internal Coordinates. *J. Phys. Chem.* **1990**, *94*, 5523−5527.
(74) Laikov, D. N.; Ustynyuk, Yu. A PRIRODA-04: a Quantum-Chemical Program Suite. New Possibilities in the Study of Molecular Systems with the Application of Parallel Computing. *Russ. Chem. Bull.* **2005**, *54*, 820−826.
(75) Evans, P. Scaling and Assessment of Data Quality. *Acta Crystallogr., Sect. D: Biol. Crystallogr.* **2006**, *62*, 72−82.
(76) (a) Battye, T. G. G.; Kontogiannis, L.; Johnson, O.; Powell, H. R.; Leslie, A. G. W. iMOSFLM: a New Graphical Interface for Diffraction-Image Processing with MOSFLM. *Acta Crystallogr., Sect. D: Biol. Crystallogr.* **2011**, *67*, 271−281. (b) Winn, M. D.; Ballard, C. C.; Cowtan, K. D.; Dodson, E. J.; Emsley, P.; Evans, P. R.; Keegan, R. M.; Krissinel, E. B.; Leslie, A. G. W.; McCoy, A.; McNicholas, S. J.; Murshudov, G. N.; Pannu, N. S.; Potterton, E. A.; Powell, H. R.; Read, R. J.; Vagin, A.; Wilson, K. S. Overview of the *CCP*4 Suite and Current Developments. *Acta Crystallogr., Sect. D: Biol. Crystallogr.* **2011**, *D67*, 235−242.
(77) Sheldrick, G. M. SHELXT − Integrated Space-Group and Crystal-Structure Determination. *Acta Crystallogr., Sect. A: Found. Adv.* **2015**, *71*, 3−8.
(78) (a) Sheldrick, G. M. A short history of SHELX. *Acta Crystallogr., Sect. A: Found. Crystallogr.* **2008**, *64*, 112−122. (b) Sheldrick, G. M. Crystal Structure Refinement with SHELXL. *Acta Crystallogr., Sect. C: Struct. Chem.* **2015**, *71*, 3−8.

DOI: 10.1021/acs.organomet.8b00363
Organometallics XXXX, XXX, XXX−XXX